

Master's Programme in Advanced Energy Solutions

Techno-economic analysis of waste heat utilization from green ammonia plant

Mikko Metsojoki

**Master's thesis
2025**

Author	Mikko Metsojoki	
Title of thesis	Techno-economic analysis of waste heat utilization from green ammonia plant	
Programme	Advanced Energy Solutions	
Major	Energy Conversion Processes	
Thesis supervisor	Prof. Ville Vuorinen	
Thesis advisor(s)	Dr Rupesh Palange	
Date	Number of pages	Language
18.7.2025	75	English

Abstract

This thesis investigated waste heat utilization from a green ammonia plant in district heat production and high temperature waste heat utilization from Haber-Bosch process in electricity generation. In addition, this thesis investigated other possible utilization alternatives for waste heat. Green ammonia is a sustainable energy carrier that is planned to be used in the future as a fuel and to replace the current use in the production of fertilizers. In this thesis, an industrial scale electric green ammonia plant was simulated with the Haber-Bosch process and an alkaline electrolyzer.

Thesis is conducted by creating a process simulation model of the green ammonia utilizing Aspen Plus software. The model was used to simulate the plant with different input powers, district heating supply temperature levels and hydrogen mass flowrates. Based on data obtained from the process simulation model. The district heating production of the plant was simulated on an hourly basis utilizing self-created MATLAB code. The simulation was carried out for two district heating networks of different sizes in Finland, which are located in potential areas in terms of plant placement. The electricity generation was separate simulation, and it was carried out only for the process simulation part.

The results indicate that the production of district heat is economically viable in term of levelized cost of heat (LCOH) in both district heating networks. However, the waste heat can only be utilized in a partially economically viable manner due to the high waste heat generation compared to the consumption in the summer months. The plant continuously generates waste heat, but its availability fluctuates greatly. The electricity production results illustrate that only small amount of electricity can be produced with Organic Rankine cycle from the high temperature waste heat. A particularly interesting finding is that the maximum electricity production is close to the rated maximum electrical power of the designed heat pumps.

Keywords green ammonia production, techno-economic analysis, waste heat utilization

Tekijä	Mikko Metsojoki
Työn nimi	Teknistaloudellinen tutkimus vihreän ammoniakki laitoksen hukkalämmön hyödyntämisestä
Koulutusohjelma	Advanced Energy Solutions
Pääaine	Energy Conversion Processes
Vastuupettaja/valvoja	Prof. Ville Vuorinen
Työn ohjaaja(t)	TkT Rupesh Palange
Päivämäärä	18.7.2025
Sivumäärä	75
Kieli	Englanti

Tiivistelmä

Tässä diplomityössä tutkittiin vihreän ammoniakki laitoksen hukkalämpöjen hyödyntämistä kaukolämmön tuotannossa ja Haber-Bosch prosessissa syntyvän korkea lämpöisen hukkalämmön hyödyntämistä sähkötuotannossa. Tämän lisäksi tutkimuksessa selvitettiin muita mahdollisia hyödyntämismahdollisuuksia hukkalämmölle. Vihreä ammoniakki on kestävä energiankantaja, jota on suunniteltu käytettävän tulevaisuudessa polttoaineena sekä korvaamaan nykyistä käyttöä lannoitteiden valmistuksessa. Tässä työssä simuloitiin teollisen mittaluokan sähköistä vihreää ammoniakki laitosta hyödyntäen Haber-Bosch prosessia ja alkalielektrolyysia.

Tutkimus toteutettiin luomalla vihreästä ammoniakki laitoksesta prosessisimulointimalli käyttäen Aspen Plus ohjelmaan. Mallia hyödyntämällä laitosta simuloitiin eri tehoilla, kaukolämmön tuloveden lämpötiloilla ja vedyn massavirroilla. Prosessisimuloinnista saadun tiedon perusteella laitoksen kaukolämmön tuotantoa simuloitiin tuntitasolla itse luotua MATLAB koodia hyödyntäen. Simulointi toteutettiin kahdelle erikokoiselle kaukolämpöverkolle suomessa, mitkä sijaitsevat potentiaalisissa alueilla laitoksen sijoittamisen kannalta. Sähkötuotanto oli täysin erillinen simulointi ja se toteutettiin vain prosessisimuloinnin osalta.

Tulokset osoittavat, että kaukolämmön tuotanto on taloudellisesti kannattavaa tasoittelujen lämmöntuotanto (LCOH) kustannusten osalta molemmissa kaukolämpöverkoissa. Hukkalämpö voidaan kuitenkin hyödyntää vain osittain taloudellisesti kannattavasti johtuen suuresta hukkalämmön tuotannosta verrattuna kesäkuukausien kulutukseen. Laitos tuottaa jatkuvasti hukkalämpöä, mutta sen saataavuus vaihtelee voimakkaasti. Sähköntuotanto tulokset osoittavat, että korkealämpöisestä hukkalämmöstä voidaan tuottaa vain suhteellisen vähän sähköä Organic Rankine kiertoprosessilla. Erityisen kiinnostava havainto on, että sähköntuotannon enimmäisteho on lähellä mitoitettujen lämpöpumppujen maksimisähkötehoa.

Avainsanat vihreä ammoniakki valmistus, teknistaloudellinen tutkimus, hukkalämmön hyödyntäminen

Table of contents

Preface and acknowledgements	7
Symbols and abbreviations	8
Symbols.....	8
Operators	8
Abbreviations	8
1 Introduction.....	9
2 Literature review.....	11
2.1 Fundamentals of water electrolysis.....	11
2.1.1 Thermodynamic.....	11
2.1.2 Electrochemistry	13
2.1.3 Electrolyzer performance and efficiency.....	15
2.1.4 Commercial electrolyzer technologies	16
2.2 Ammonia production.....	20
2.2.1 Industrial scale ammonia synthesis.....	21
2.3 Energy flows in green ammonia production	23
2.4 Waste heat utilization and conversion	27
2.4.1 District heating network.....	30
2.4.2 Industrial heat pumps	33
2.4.3 Organic Rankine cycle	36
3 Green ammonia plant model	39
3.1 Alkaline electrolyzer model.....	39
3.2 Haber-Bosch model.....	41
3.3 Electricity generation model.....	42
3.4 Heat Pump model.....	43
4 Research material and methods.....	45
4.1 Input data	45
4.2 Parametric calculations	48
4.2.1 Aspen Plus.....	48
4.2.2 Programming	49
4.3 Levelized cost modelling.....	51

5	Results and discussion	54
5.1	Model validation	54
5.2	Parametric simulation	56
5.3	Levelized cost of heat	62
5.4	Electricity generation.....	63
5.5	Limitations of the thesis	64
6	Conclusions	65
	References.....	67
	Appendix.....	75

Preface and acknowledgements

This thesis was conducted as part of AINA research project which provided this relevant and fascinating topic. I would like to thank than my thesis supervisor Prof Ville Vuorinen and advisor Dr Rupesh Palange for their excellent feedback and guidance throughout the thesis. I am also grateful to Kokkola Energia and Oulu Energia for providing the district data since without the data thesis would have not been possible in this extend.

Espoo 18th July 2025
Mikko Metsojoki

Symbols and abbreviations

Symbols

E	Energy
F	Faraday constant
G	Gibbs energy
H	Enthalpy
I	Current
n_t	Thermal efficiency
Nm ³	Normal cubic meter
P	Power
r	Discount rate
Q	Heat
t	Time
T	Temperature
U	Voltage
W	Work

Operators

Δ	Change
Σ_i	Sum over index i

Abbreviations

AEL	Alkaline electrolyzer
CAPEX	Capital expenditure
COP	Coefficient of performance
DH	District heating
GWP	Global warming potential
HHV	Higher heating value
KOH	Aqueous potassium hydroxide
LCOH	Levelized cost of heat
LHV	Lower heating value
ODP	Ozone depletion potential
OPEX	Operational expenditure
ORC	Organic Rankine cycle
PEMEL	Proton exchange membrane electrolyzer
PPA	Power purchase agreement
SG	Safety ground
TRL	Technical readiness level

1 Introduction

Green ammonia refers to ammonia produced entirely from renewable energy sources relying only water, air and power (Salmon & Bañares-Alcántara, 2022). This concept of green ammonia production with Haber Bosch process is not a new technology since dates to 1928 when it was firstly implemented in industrial scale using hydropower (Rouwenhorst et al, 2022). Already back then, the most important feedstock of the process hydrogen was generated by alkaline electrolyzer. Currently, the synthesis of ammonia relies on same famous process called Haber-Bosch, but hydrogen production relies almost exclusively on fossil feedstocks. In recent years, interest in green ammonia has increased due to its potential as carbon free energy carrier, a sustainable fuel for transport sector and replacement for current fossil fuel-based fertilizer production (Bora et al, 2024). This trend is also evident in Finland where several plans are underway to construct green ammonia plants (EK, 2025).

Green ammonia production generates waste heat as a byproduct making it as noteworthy low carbon heat source. When powered by wind power green ammonia achieves a low carbon intensity of $0,38 - 0,53 t_{CO_2-eq}/t_{NH_3}$ compared to $1.673 t_{CO_2-eq}/t_{NH_3}$ for modern methane-based production (Smith et al, 2020). Therefore, the waste heat from green ammonia production is attractive in solution for Finland where cold climate with extensive district heating networks enables exceptionally well large-scale utilization of waste heat. In addition, Finland has an ambition carbon neutrality target by 2035 (Finlex, 2022). Similarly, district heating relies heavily on biofuel with share of 48 % of district heat production in Finland (Finnish energy, 2024). This raises the question of whether the utilization of this byproduct could be economically viable for ammonia plant operators while simultaneously supporting Finland achieving its carbon neutrality target. Furthermore, what other potential alternatives exist for the utilization of the waste heat?

In this thesis, an electric green ammonia plant is modelled with Aspen Plus containing following parts of the plant alkaline electrolyzer, heat pump and Haber-Bosch process. Target of this thesis is to investigate industrial scale green ammonia plant waste heat utilization in district heating network and examine other possible applications for the waste heat. Electricity generation from high-temperature waste heat of Haber-Bosch process is a topic that has received limited attention in the academic literature with only one paper by Anwar et al. (2024) addressing the subject previously. Therefore, this thesis aims to examine this topic with greater extent.

Research questions of thesis are following.

1. Create a model of green ammonia plant
2. Examine different applications for the waste heat utilization in literature review.
3. Find feasible size for the heat pump in given scenarios.
4. Calculate levelised cost of produced district heat.
5. Demonstrate electricity generation potential from high temperature waste of Haber-Bosch process.

2 Literature review

Literature review part covers basic theory related to water electrolysis, green ammonia production and waste heat recovery. Secondly, waste heat generation of green ammonia production is explained and important equations are related topic are presented in this chapter. Finally, potential consumers and conversion technologies utilized in this thesis for the waste heat recovery are examined.

2.1 Fundamentals of water electrolysis

Water electrolysis is method where water molecules are separated into hydrogen and oxygen driven by electric current. The reaction occurs on two electrodes in an electrolyte which raises ionic conductivity. Hydrogen is generated at the cathode side where reduction half reaction occurs. Oxygen is generated at the anode side where oxidation half-reaction occurs. Hence, anode is positive polarized, and cathode is negative polarized. Between electrodes there is diagram of separator which prevents the recombination of generated oxygen and hydrogen. Equation 1 illustrates the overall reaction of electrochemical water splitting into hydrogen and oxygen. Regardless of technology this equation below applies for all technologies. (Ursua et al, 2011)

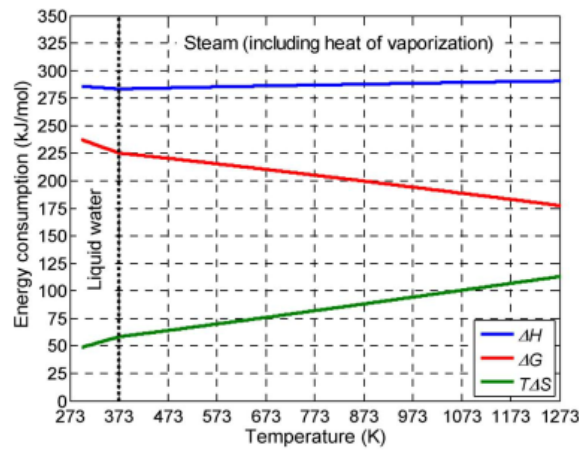


2.1.1 Thermodynamic

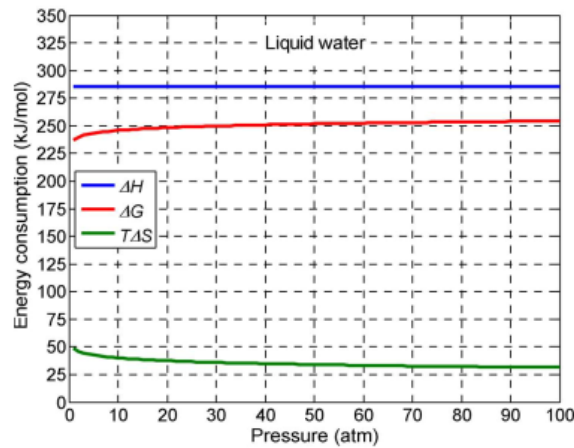
Total energy required to split one mole of water molecules can be calculated from Gibbs-Helmholtz equation for given pressure and temperature presented in equation 2 (Buttler & Spliethoff, 2018). Where ΔH denotes to enthalpy change, ΔG denotes to change in Gibbs free energy change and ΔS denotes to change in entropy. Reaction requires to occur both electric and thermal energy. Gibbs free energy change ΔG corresponds the required electric part of the total energy and product of process temperature (T) and entropy change ΔS covers rest of energy required as thermal energy. The water electrolysis is endothermic and nonspontaneous chemical reaction. At standard temperature of 298,15 K and pressure of 1 atm, $\Delta G^0 = 237,21 \frac{kJ}{mol}$, $\Delta S^0 = 0,1631 kJ/mol$ and $\Delta H^0 = 285,84 kJ/mol$. (Ursua et al, 2011)

$$\Delta H(T, P) = \Delta G(T, P) + T\Delta S(T, P) \quad (2)$$

Figure 1 illustrates how the total energy consumption of an ideal electrolysis process varies depending on pressure and temperature. According to figure 1a total energy consumption decreases slightly in the liquid state as temperature increases. In contrast, total consumption slightly increases in the gaseous state. However, total electric energy demand decreases, and thermal energy demand increases in both state when temperature increases.



(a)



(b)

Figure 1. Influence of temperature and pressure to an ideal electrolysis process energy consumption. Figure 1a as function of the temperature at standard pressure. Figure 1b as function of the pressure at standard state. (Ursua et al, 201)

Figure 1b indicates that total energy consumption remains almost as constant despite the pressure increase. Decrease in total energy consumption is only 0,03 % when pressure is increased from 1 to 100 atm (Ursua et al, 2011). Electric energy demand increases by 7,3 % and in contrast, thermal energy demand decreases by 35,5 % as pressure rises from 1 to 100 atm (Ursua et al, 2011). Hence, balancing total energy consumption of electrolysis reaction.

Reversible voltage presented in equation 3 is the lowest voltage where water splitting can occur where change in Gibbs energy is directly proportional to voltage, z denotes to number of electrons transferred in the reaction ($z = 2$) and F denotes to Faraday's constant (96 485 C/mol). It describes the necessary external heat demand to cover whole heat demand. (Buttler & Spliethoff, 2018) At standard conditions, reversible voltage is 1,229 V (Ursua et al, 2011).

$$U_{rev} = \frac{\Delta G}{zF} \quad (3)$$

Thermoneutral voltage describes minimum voltage required for ideal cell to water electrolysis to occur without external heat source in adiabatic conditions when all energy is provided purely as electricity to system (Sánchez et al, 2020). Equation for thermoneutral voltage is illustrated in equation 4. At standard conditions, thermoneutral voltage is 1,481 V (Ursua et al, 2011).

$$U_{tn} = \frac{\Delta H}{zF} \quad (4)$$

2.1.2 Electrochemistry

In commercial electrolyzers, measured cell voltage is slightly higher than thermoneutral voltage due to thermodynamic irreversibilities and heat losses in the system (Ursua et al, 2011). In addition, thermoneutral describes standard operation conditions of high temperature electrolyzers at constant operation conditions where heat consumption of reaction equals with internal heat production. However, low temperature electrolyzers such as alkaline and proton exchange membrane are operated higher cell voltages than thermoneutral voltages due to overvoltage's or high internal losses. Hence, waste heat is generated in electrolyzer cell, and this waste heat must be removed from the cells to maintain constant operating conditions (Buttler & Spliethoff, 2018). Equation 5 represents theoretical equation for evaluation of the waste generation which is directly proportional to difference between cell voltage and thermoneutral voltage where N denotes number of cells in a single stack, and I denotes to current. Heat transfer losses are neglected in this equation 5 and net amount of excess heat is given by equation 6. (Sánchez et al, 2020)

$$Q_{gen} = NI(U_{cell} - U_{tn}) \quad (5)$$

$$Q_{excess} = Q_{gen} - Q_{loss} \quad (6)$$

Calculation principle of cell voltage is illustrated in equation 7 where cell voltage is sum of reversible voltage U_{rev} , overvoltages caused by ohmic losses U_{ohm} , activation overvoltages U_{act} and concentration overvoltages U_{con} (Ursua et al, 2011).

$$U_{cell} = U_{rev} + U_{ohm} + U_{act} + U_{con} \quad (7)$$

Operating conditions have influence on waste heat generation from the electrolyzer stacks. Adibi et al (2022) have modelled different operating conditions on commercial alkaline electrolyzer at unsteady state. Results of Adibi et al (2022) indicate that different operating conditions such as temperature, current and pressure have influence on cell voltage, thermoneutral voltage and Faraday's efficiency. Figure 2 illustrates temperatures effect on the cell voltage as function of current. It can be observed from figure 2 that the cell voltage increases when temperature decreases or current increases. In contrast, pressure effect to cell voltage variation between different pressure levels is small compared to temperature effect. However, the cell voltage slightly increases with higher pressure levels. (Adibi et al, 2022)

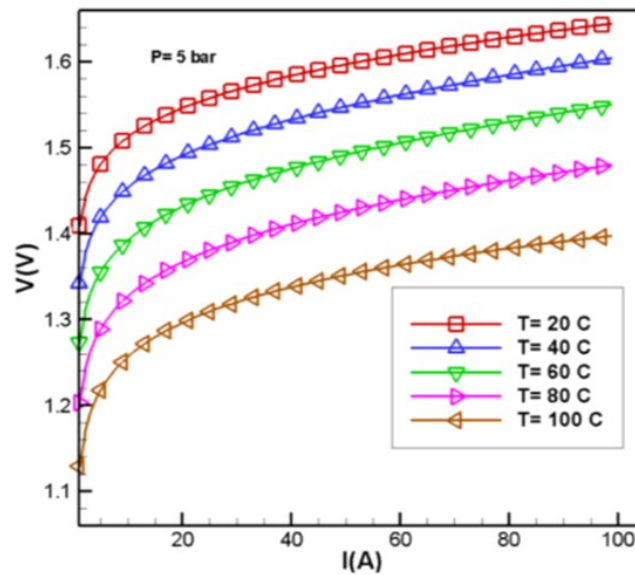


Figure 2. Influence of temperature to alkaline electrolyzer cell voltage versus electrical current (Adibi et al, 2022).

Since heat generation of alkaline electrolyzer depends on the difference between the thermoneutral voltage and the cell voltage. When operating temperature of electrolyzer increases the thermoneutral voltage increases and the cell voltage decreases. Resulting to smaller difference between the thermoneutral voltage and the cell voltage. Therefore, raising temperature of the

electrolyzer results to reduced heat generation from the stack. In contrast, thermoneutral voltage decreases as pressure increases. (Adibi et al, 2022)

2.1.3 Electrolyzer performance and efficiency

Power of stack can be determined according to equation 8 where I_{cell} indicates to current density (Sánchez et al, 2020). A single stack consists of multiple cells connected series and multiple stacks can be connected parallel in an electrolysis plant. Hence, total power of the plant is defined as sum of stack powers.

$$P_{stack} = U_{stack}I = U_{cell}NI_{cell}A_{cell} \quad (8)$$

The hydrogen production rate can be determined according to equation 9 where n_f denotes to Faraday's efficiency. This parameter is defined ratio between actual hydrogen production and the theoretical hydrogen production in moles. As equation 9 represents hydrogen production rate is directly proportional to power applied to stack. Consumption of water and production of water can be determined from reaction stoichiometry. Equations 10-11 presents mass balances for electrolysis cell. (Sánchez et al, 2020)

$$n_{H_2,prod} = n_f \frac{IN}{zF} \quad (9)$$

$$n_{O_2,prod} = \frac{1}{2} n_{H_2,prod} \quad (10)$$

$$n_{H_2O} = n_{H_2,prod} \quad (11)$$

There are many different methods to define water electrolyzer efficiency since it can be defined for system level or on stack level or from specific energy consumption perspective. On the system level the energy efficiency can be defined according to equation 12 where V_{H_2} denotes hydrogen production rate of an electrolyzer, HHV_{H_2} denotes to higher heating value of hydrogen which is 3,54 kWh/Nm³ and P_{el} denotes to total electric power of an electrolyzer systems in kW (Buttler & Spliethoff, 2018).

$$n_{HHV} = \frac{V_{H_2} HHV_{H_2}}{P_{el}} \quad (12)$$

Voltage efficiency is another commonly utilized parameter to measure the energy efficiency of water electrolyzer. Equation for voltage efficiency is

presented in equation 13 as ratio between thermoneutral voltage and actual cell voltage. This equation represents conversion efficiency of electrical energy to chemical energy (Kumar & Himabindu et, al 2019). In general, efficiency of an electrolyzer decreases when temperature decreases, current density or pressure increases due to increase in overvoltages. However, effect of pressure increase is only slight to efficiency. (Buttler & Spliethoff, 2018)

$$n_v = \frac{U_{tn}}{U_{cell}} \quad (13)$$

Thirdly, specific energy consumption is another commonly utilized parameter for electrolyzer efficiency. This parameter represents ratio between energy consumed to produced hydrogen commonly expressed in kWh/Nm³ Equation 14 presents equation for specific energy consumption for a stack where f_{H_2} denotes to volumetric hydrogen production rate in Nm³/h. (Ursua et al, 2011)

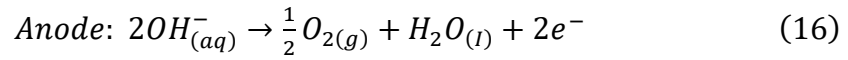
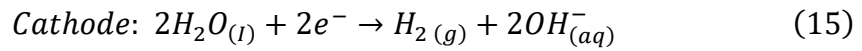
$$E_s = \frac{\int_0^t NIU_{cell} dt}{\int_0^t f_{H_2} dt} \quad (14)$$

Electrolyzer efficiency can be defined by utilizing lower- or higher heating values of hydrogen which are utilized to present chemical energy content of fuels. Hydrogen higher heating value (HHV) for hydrogen is 39,4 kWh/kg or 141,8 MJ/kg and lower heating value (LHV) is 33,3 kWh/kg or 120 MJ/kg (van der Roest et al, 2023). In case of electrolyzer, HHV should be selected to avoid over estimating waste heat potential of an electrolyzer. Hence, electrolysis is electrochemical energy conversion method where burning is not involved. Since LHV is only relevant in cases where substances are burned, and no heat recovered from flue gages. Therefore, HHV of hydrogen represents better the amount of potential waste heat from an electrolyzer. (van der Roest et al, 2023)

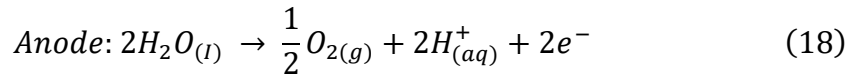
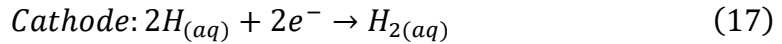
2.1.4 Commercial electrolyzer technologies

There are currently four utilized water electrolyzer technologies on the market. These are alkaline electrolysis (AEL), proton exchange membrane electrolysis (PEMEL), anion exchange membrane electrolysis (AEMEL) and Solid oxide electrolysis (SOE) which are classified according to the applied electrolyte. In addition, technologies differ in operating temperature range and the inions exchanged in the reactions. Hence, technologies have different efficiencies, purity levels of products and requirement for the reactants. (Lange et al, 2023)

Currently, AEL and PEM are the only commercial electrolyzer technologies with high technology readiness levels and both technologies are suitable for this master thesis application and from the research questions perspective due to low operation temperature of both technologies (David et al, 2019). AEL is mature widespread commercial technology where electrodes are immersed in a liquid electrolyte with usual concentration of 25-30 w% aqueous potassium hydroxide (KOH). The electrodes are separated by a diaphragm. (Buttler & Spliethoff, 2018) Partial reactions of AEL are given in equations 15-16 (David et al, 2019).



In Polymer Electrolyte Membrane or Proton Exchange Membrane (PEM) electrolyzer, electrodes are separated by solid exchange membrane usually made of Nafion®. Furthermore, electrodes are typically directly mounted against the membrane. (Buttler & Spliethoff, 2018) On other hand, PEM includes expensive noble and rare metals such as platinum at cathode and iridium at anode which can be considered hinder the large-scale utilization of this technology (Zhang et al, 2022). Partial reactions of PEM electrolyzer are presented in equations (17-18) (David et al, 2019).



Typical water electrolysis plant consists of multiple identical stacks connected parallel which can be operated individually. Figure 3 illustrates a schematic flow diagram of an AEL stack. Circulating electrolyte flow is pumped through the electrolysis stack where the split reaction of water occurs. Then, both product gases and two-phase mixture of liquid electrolyte flows from stack to gas separator where two phase are split. This splitting occurs in large tanks with long residence time. After gas separators, the liquid phase electrolyte cycles back to the electrolysis stack and product gases enter to demister and dryer before final purification. Liquid electrolyte flows from gas separators are mixed at equalization line to maintain optimal electrolyte conductivity, mass-and energy balances of the system. Mixing of the electrolytes is required since without mixing concentration of electrolyte would change. (Brauns & Turek, 2020) Purpose of heat exchangers is to

remove excess heat generated inside an electrolyzer cell stack and maintain electrolyzer temperature as a constant. (Sakas et al, 2022)

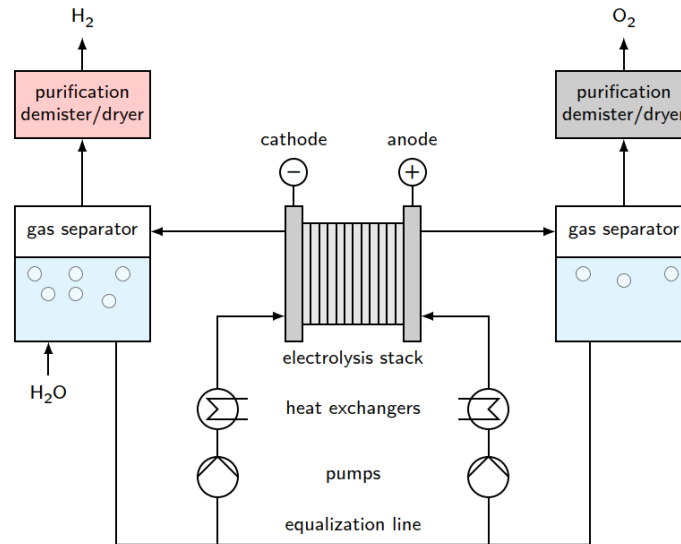


Figure 3. A schematic flow of diagram of an alkaline electrolyzer (Brauns & Turek, 2020).

Table 1 summaries technical characteristics and flexibility parameters of AEL and PEM electrolyzers from literature. All flexibility parameters presented in table 1 are illustrating the flexibility values of an electrolyzer stack. Load flexibility denotes to partial load range of a stack compared to specified nominal power of the stack. Heat-up ramp is a parameter that illustrates the temperature gradient limit for heating of the stack into the operating temperature. (Lange et al, 2023) Warm start-up time of electrolyzer describes time required electrolyzer reach to full load from stand-by mode when electrolyzer is heated and pressurised (Buttler & Spliethoff, 2018).

Table 1 Summary of technical characteristics and flexibility parameters of AEL and PEM electrolyzers.

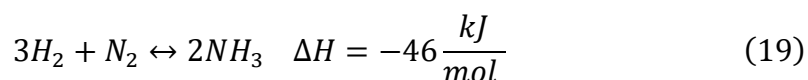
Specification	AEL	PEM	Reference
Cell temperature (°C)	60-90	50-80	Buttler & Spliethoff, 2018
Cell pressure (bar)	<= 30	<80	David et al, 2019 & Buttler & Spliethoff, 2018, Lange et al, 2023
Current density (A/cm ²)	< 0,45	0,8-2,5	David et al, 2019, Lange et al, 2023
Cell voltage (V)	1,8-2,4	1,8-2,2	David et al, 2019
Cell area (m ²)	< 3,6	<0.13	Buttler & Spliethoff, 2018
Voltage efficiency (%)	62-82	67-82	David et al, 2019
Nominal stack efficiency (LHV %)	63-71	60-68	Buttler & Spliethoff, 2018
Specific energy consumption stack (kWh/Nm ³)	4,2-4,8	4,4-5,0	Lange et al, 2023
Stack lifetime (kh)	55-120	60-100	David et al, 2019
System lifetime (year)	20-30	10-20	David et al, 2019
Efficiency degradation (%/a)	0,25-1,5	0,5-2,5	Buttler & Spliethoff, 2018
Hydrogen purity (%)	> 99,8	99,999	David et al, 2019
Investment cost (€/kW)	800-1500	1400-2100	Buttler & Spliethoff, 2018
Maintenance cost (% of investment cost)	2-3	3-5	Buttler & Spliethoff, 2018
Load flexibility (%)	20-100	0-160	Lange et al, 2023
Cold start-up time (o-load) (min)	5-15	<10-15	Lange et al, 2023
Warm start-up time (standby to full load) (min)	1-5 min	<10 s	Lange et al, 2023
Heat-up ramp (K/min)	0,4-15	0,3-1	Lange et al, 2023
Load gradient power increase (%/s)	10-50	10-90	Lange et al, 2023
Load gradient shut-down (%/s)	10	40,6	Lange et al, 2023

For flexible operations with renewable power source PEM is more suitable technology than AEL due to better flexibility parameters illustrated in table 1. On the other hand, PEM is more expensive technology, with higher degradation rate and shorter lifetime. In the future, it is expected that both electrolyzer technologies current densities to improve, degradation rate and specific energy consumption to reduce (Lange et al, 2023).

2.2 Ammonia production

Ammonia is an important organic chemical that exist as colourless gas with pungent odour at standard conditions. Density of ammonia is a bit lower than air and boiling of ammonia is $-33,4\text{ }^{\circ}\text{C}$ at atmospheric pressure. (Chehade & Dincer, 2021) From safety perspective, ammonia is toxic chemical for humans and animals depending on concentration of ammonia in the air (Chehade & Dincer, 2021). Majority of produced ammonia is utilized as feedstock for production of nitrogenous fertilizers (Bora et al, 2024). Therefore, ammonia production has important role in the modern world agricultural.

Equation 19 illustrates the reaction for the synthesis of ammonia from unreactive nitrogen and hydrogen (Rouwenhorst et al, 2022). In this reaction, hydrogen and nitrogen reacts with ratio of 3:1 under high pressure and temperature. Negative value of ammonia formation indicates that reaction is exothermic. Hence, resulting heat generation of approximately 2,7 GJ per tonne of ammonia produced (Ruddock & Brudenell, 2003).



Currently, the most widely utilized process to produce ammonia is the Haber-Bosch process (Chehade & Dincer, 2021). Hence, 90 % of worldwide ammonia production is covered by Haber-Bosch process (Osman et al ,2020). Advantages of Haber-Bosch include maturity, reliability and high optimization factor of the process when disadvantages include aspect such as high operating pressure and non-modularity. (Cameli et al, 2024)

There are many different feedstocks for ammonia production such as natural gas, coal, biomass, heavy fuel oil, naphtha and renewables. Currently, ammonia production is based almost exclusively on natural gas and coal as feedstocks. (Rouwenhorst et al, 2022) However, green ammonia can be produced via multiple different conversion technologies such as electric Haber-Bosch, electrochemical, non-thermal plasma, photocatalytic, metallocplexes and biological. Figure 4 illustrates process flow sheet of electric green ammonia production plant and gas temperature in different stages of the process. In the electric ammonia plant, hydrogen is produced by water electrolysis and nitrogen is produced utilizing an air separation unit. The Haber-Bosch process generates high temperature waste heat while electrolyzer generates low temperature waste heat as byproducts. (Chehade & Dincer, 2021)

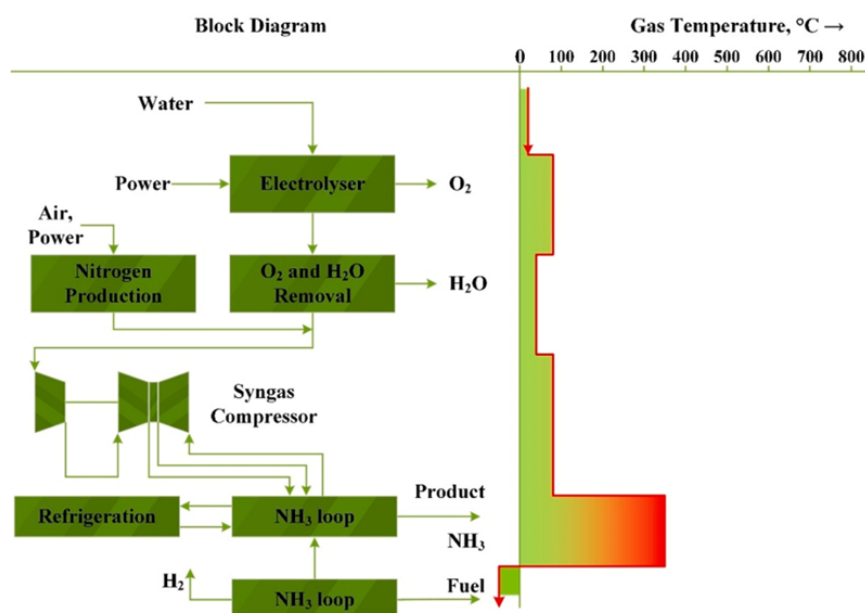


Figure 4. Process flow sheet of green ammonia production plant (Chehade & Dincer, 2021)

From technical readiness level (TRL) perspective, electric Haber-Bosch with AEL or PEM electrolyzer can be identified as most promising technologies for green ammonia production in the near future compared to other alternative technologies. TRL for electric Haber-Bosch with AEL is 8-9 and for high pressure PEM it is 6-7 (Smith et al, 2020).

2.2.1 Industrial scale ammonia synthesis

Currently, large-scale ammonia production relies purely on the Haber-Bosch process with typical production capacity over 200 kt of ammonia annually (IEA, 2021). Large-scale Haber-Bosch process operating conditions ranges between 150-250 bar and 400-550 °C and process operates typically with presence of iron-based catalyst (Cheema & Krewer, 2018). Operating

conditions of ammonia synthesis are trade of between pressure and temperature since high inlet temperature is needed to achieve high reaction rates. On the other hand, low outlet temperature is referred to achieve high equilibrium conversion. Hence, multiple catalyst beds are connected in series with intermediate cooling to achieve high reactant conversion in the ammonia synthesis. (De la Hera et al, 2024)

Figure 5 illustrates simplified diagram of conventional high pressure ammonia synthesis process where ammonia is produced at high pressure and ammonia separation from unreacted gases occurs in phase-charging condensation (Lin et al, 2020). The model presented in figure 5 includes five main elements in typical Haber-Bosch plant such as a compressor, a heat exchanger, an ammonia separation system, a recycle stream and a purge stream (De la Hera et al, 2024).

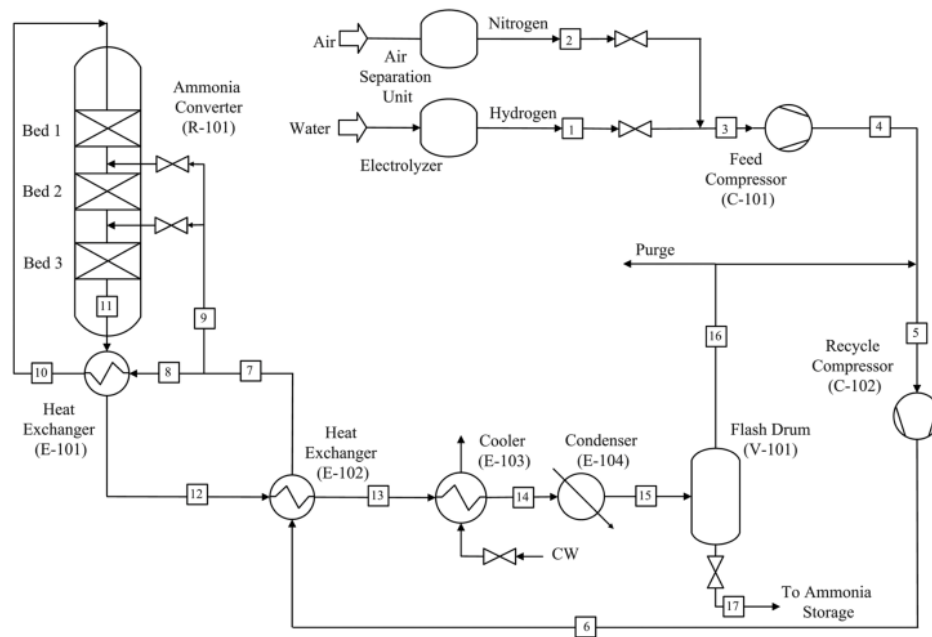


Figure 5. Simplified schematic diagram of ammonia production with conventional high-pressure reaction-condensation (Lin et al, 2020).

Ammonia plant is fed by high purity elements which purity requirements are following 99,999 % for hydrogen and 99,99 % for nitrogen (Osman et al ,2020). Fed nitrogen and hydrogen are firstly compressed and mixed with recycled stream. Then, the mixed stream is further compressed and preheated with waste heat from reactor before the stream fed into multistage bed reactor where reaction occurs. After the reactors, output stream is cooled by the heat integration exchangers. Then, output stream is further cooled, and ammonia is separated by condensation from untreated hydrogen and nitrogen. Condensation separation is typical solution for ammonia extraction

with traditional high-pressure ammonia synthesis due to efficiency reasons. With low pressure ammonia synthesis absorption separation is utilized. (De la Hera et al, 2024)

Produced liquid ammonia flows into ammonia storage tank with typical industrial purity level of 99,5 % (Morgan et al, 2017). Unreacted gases are recirculated back to reactor since single pass conversion rate of ammonia is limited between 15-30 % in commercial plants due to unfavourable equilibrium condition in the reactors (Chehade & Dincer, 2021). Lastly, purpose of purge stream is to remove inert gases by purging a small amount of the recycling stream out of the synthesis loop to avoid build-up of inert gases into the synthesis loop. In conventional ammonia synthesis based on steam methane reforming inert gases are argon and methane. In this thesis power-to-ammonia type synthesis, only inert gas is argon. (Cheema & Krewer, 2018)

Wang et al (2023) have researched flexibility data of large-scale Haber-Bosch reactors and have concluded that there is not enough knowledge about reactors flexibility since existing reactors are not originally designed for flexible operations. All knowledge of flexibility is based on dynamic simulations in literature or from small scale demonstrations where the minimum load ranges between 20 % to 60 % of the nominal feedstock load (Wang et al, 2023).

Variation of feedstock flow are not harmless for the process since variation can lead to efficiency deterioration, system instabilities and unwanted operation deviations. Especially ramping down feedstock influences harmfully to integrity of the catalyst since ramping down disturbs the process operating temperature. Hence, the temperature management is considered as main limiting factor in load range of Haber-Bosch process. (Wang et al, 2023)

2.3 Energy flows in green ammonia production

In general, green ammonia production is a very energy intensive process where the most efficient electrolyzer-based ammonia production consumes around 33 GJ/t-NH₃ currently (Rouwenhorst et al, 2022). Figure 6 presents development in energy consumption for coal-based ammonia synthesis, electrolysis-based ammonia synthesis, and natural gas-based ammonia synthesis. Electricity consumption of water electrolysis-based ammonia production is dominated by hydrogen production by share of 80-90 % (Collando et al, 2024). According to De la Hera et al (2024) simulation results AEL covers 80,6% of total electricity consumption, followed by Haber-Bosch process for ammonia production which share was 18,6 % with operating pressure of 205 bar and for nitrogen production share was just 0,818 %.

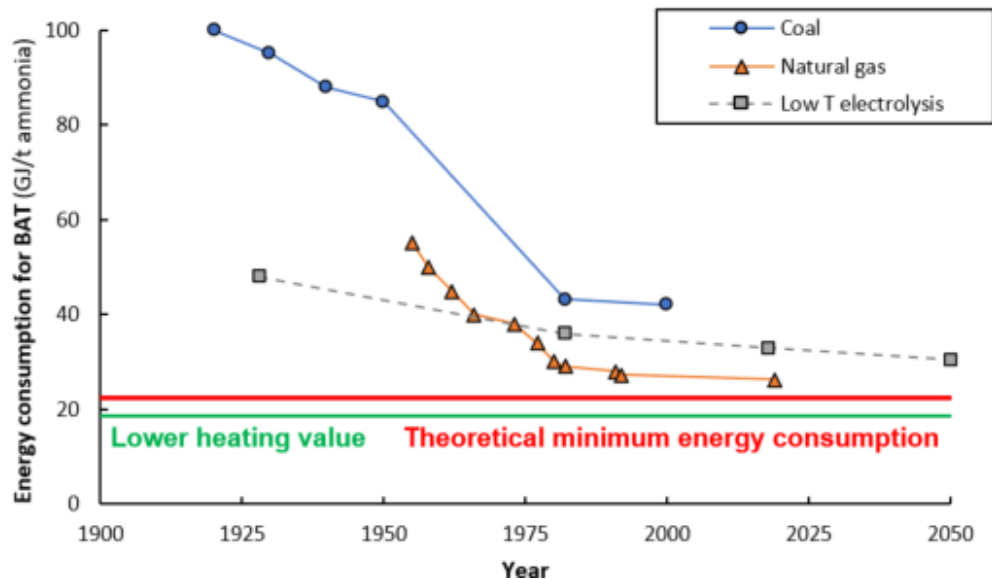


Figure 6 Comparison of energy consumption of different ammonia synthesis technologies. Bat refers to best available technology (Rouwenhorst et al, 2022).

Sakas et al (2022) have modelled an industrial alkaline electrolyzer power distribution in stack and in system level. Result presented in figure 7 are validated against real electrolyzer with 98,7 % accuracy for temperature of stack in dynamic operations. At steady state, 11,2 % of the supplied power is consumed by the shunt currents, 20,3 % is lost due to ohmic and activation overvoltages and rest 68,5 % supplied power is converted into hydrogen. Heat losses are calculated to be 2,64 % from the stack into ambient air and 0,3 % is removed by oxygen and hydrogen streams flowing out of the system. Rest of the excess heat is extracted by heat exchangers on anode and cathode sides. Furthermore, part of produced hydrogen is lost in the process since 0,4 % is burned in deoxidizer in the purification of hydrogen and 2,5 % is lost to gas impurities related diagram diffusion and process mixing. (Sakas et al, 2022)

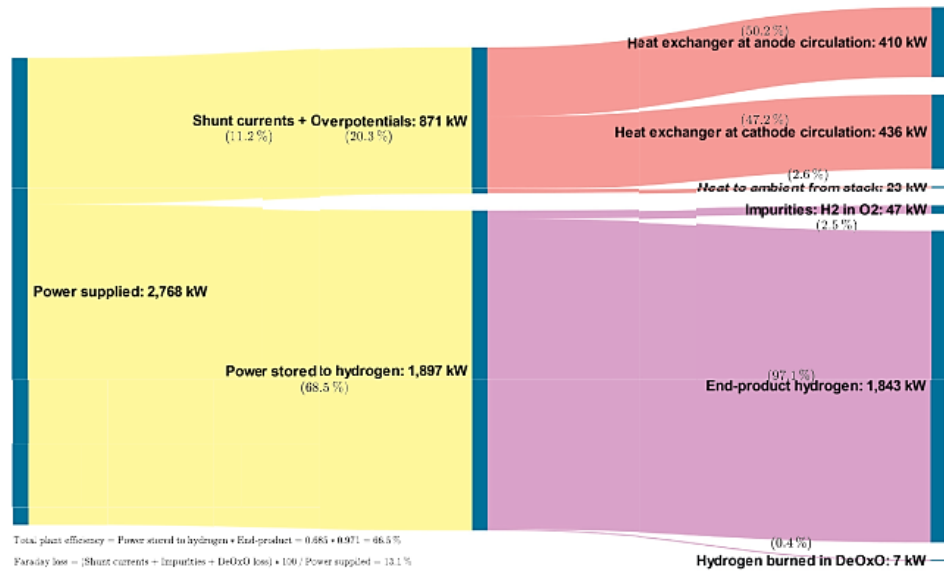


Figure 7 Power flow diagram of an AEL (Sakas et al, 2022).

Smit et al, 2020 have calculated and compared energy losses between current steam reforming based- and future electrically driven Haber-Bosch processes which results are presented in figure 8. Results indicate majority of energy losses in electrically driven technologies occur in hydrogen production due to low efficiency of water electrolysis.

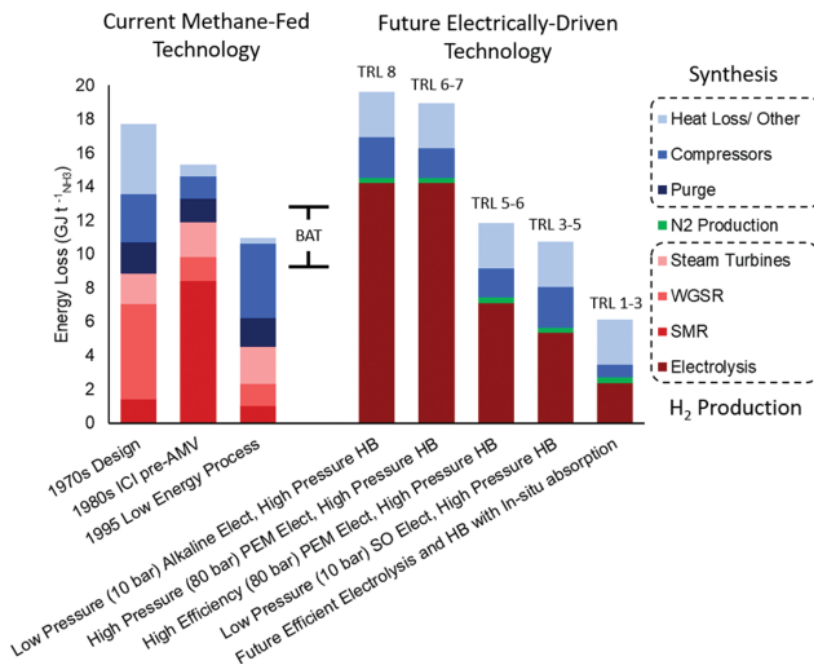


Figure 8 Comparison of current methane-fed and electrified Haber-Bosch processes energy losses (Smith et al, 2020).

Furthermore, figure 8 illustrates that nitrogen production share of total energy losses is rather insignificant. On other hand, energy losses from ammonia synthesis loop are lower with electrically driven compared to 1995 low energy process. Reduction is caused by three main reasons according to Smit et al, 2020. Firstly, energy required for compression reduces since an electrolyzer can produce hydrogen under pressure. Secondly, purge from synthesis loop can be ignored due to high purity of hydrogen and nitrogen. Thirdly, energy losses are reduced since compressor are powered with more efficient electric motors than steam turbines. In current technology, steam turbines are driven by waste heat from steam reforming reactors and therefore low efficiency steams turbines are utilized to power compressors. (Smith et al, 2020)

Anwar el al (2024) have investigated waste heat recovery from electric green ammonia production with Kalina cycle and a vapour absorption refrigeration conversion cycle. Result of this research are presented in figure 9 and electrolyser technology utilized in this study is AEL. In the Kalina cycle, waste heat is partly converted back to electricity and rest of thermal energy is utilized as heat. In the vapour absorption refrigeration cycle, final products are waste heat and refrigeration.

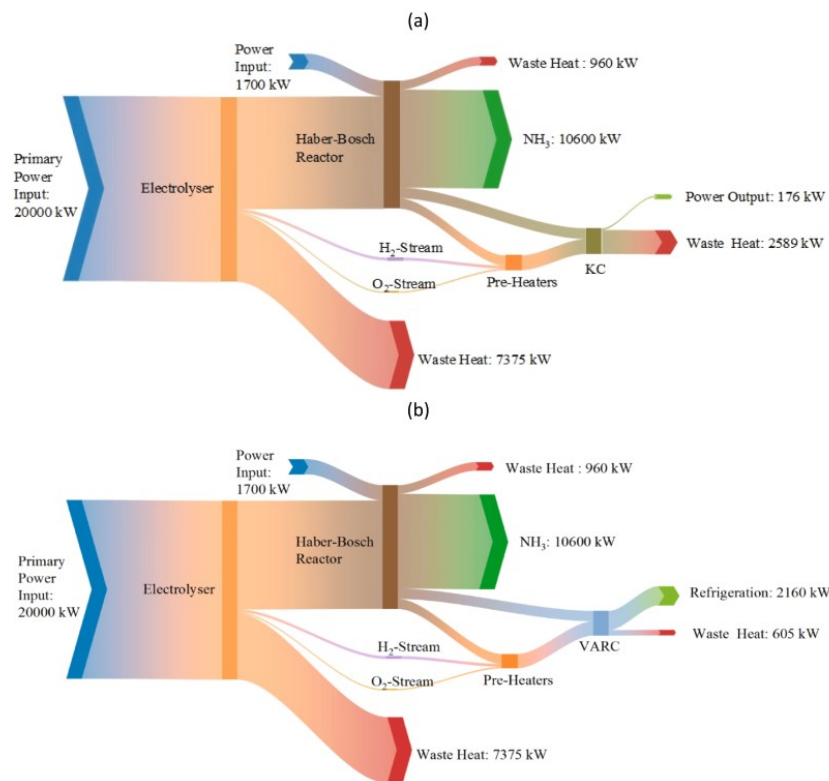


Figure 9. Energy flow charts of green ammonia plant with Kalina heat recovery (a) and vapour absorption refrigeration cycle (b) (Anwar et al, 2024).

40 % of input power is dissipated to waste heat during water electrolysis according to result presented in the figure 9. Heat is released mainly during the separation phase while only small amount of recycling water converts to hydrogen during one cycle. However, only small fraction of this low temperature waste heat from electrolyzer can be utilized in both heat recovery technologies due to high operating temperatures of Kalina and vapour absorption refrigeration cycle compared to AEL. The rest of energy losses occur in ammonia synthesis in the Haber-Bosch system where 24 % of the input power is dissipated to waste heat. Thermal losses in Haber-Bosch process are caused by post-ammonia formation and separation due to high operation temperature and pressure condition required in the process. (Anwar et al, 2024)

2.4 Waste heat utilization and conversion

Utilization of waste heat from water electrolysis and ammonia synthesis for district heating (DH) networks is well recognized concept in the literature (Smit et al, 2019). This waste can be utilized in DH network directly or by upgrading the heat temperature. Several authors have conducted techno-economic evaluations of utilization of waste heat from water electrolysis with heat pumps for DH applications. Meriläinen et al (2024) have investigated of the utilization of waste heat from off-grid AEL powered by wind power and photovoltaics for DH network under southeastern Finland weather conditions. Setup of this study included heat pumps to raise temperature waste heat to suitable for DH network, a pit thermal storage operating as seasonal storage and an electric boiler as additional heat source. The results of Meriläinen et al (2024) showed that levelized cost of heat (LCOH) ranges from about 16 €/MWh to 44 €/MWh when coverage rate of DH demand ranged from about 25% to 100%. Furthermore, illustrated that heat pumps have largest influence on LCOH by share up to 50% (Meriläinen et al, 2024).

In another study, waste heat utilization was examined from small a 2,5 MW PEM electrolyzer with and without utilization of heat pump in the Netherlands. In this study, electrolyzer was powered by local photovoltaics and during low spot electricity prices by grid power. The results demonstrated that without heat pump LCOH is 8,9 €/MWh when temperature of feedwater is set 54 °C for the low temperature DH network. With heat pump LCOH was calculated to be 36,9 €/MWh with feedwater temperature set to 100 °C. (van der Roest et al, 2023) In addition, both cases are recognized be to economically feasible options compared to other low or high temperature heat sources according to comparison of van der Roest et al (2023).

Industrial sector is also potential consumer for the waste from green ammonia plant. Literature have identified the most potential industrial sectors that can utilize large amount of within temperature range 100-200 °C such as food, paper, iron and steel, chemical, and non-metallic mineral industries (Kosmadakis, 2019). This temperature band is also partly achievable with current industrial heat pumps. However, these potential industries also reject large amount waste heat themselves that can utilized to as heat source for industrial heat pumps. (Kosmadakis, 2019) From the food industry, the literature suggests especially heated greenhouses as a potential consumer for the waste heat generated in ammonia synthesis (Smith et al, 2020). Table 2 presents simulated heating consumption in a greenhouse where tomatoes are grown. The simulation results are based on meteorological data 1973-2014. (Mariani et al, 2016)

Table 2. Simulated greenhouse heating consumption in Närpes Finland. (Mariani et al, 2016).

Time period	Average (MJ/m²)	Standard deviation (MJ/m²)
Year	2058	165
Dec-Fed	1056	139
Mar-May	505	53
Jun-Aug	49	12
Sep-Nov	450	74

Similarly, table 3 illustrates some example processes from different industrial sectors where waste heat could be utilized and typical temperature range for the processes. In addition, public swimming baths located in swimming halls are common high energy consumers in Finland. Saari & Sekki 2008 have calculated that the annual energy consumption of one recently built public swimming pool was 396 kWh/m² in 2008.

Table 3 Processes of different industrial sectors and typical temperature ranges (Arpagaus et al, 2018).

Sector	Process	Temperature (°C)
Paper	Drying	90-240
	Boiling	110-180
	Bleaching	40-150
	De-inking	50-70
Food and Beverages	Drying	40-250
	Evaporation	40-170
	Pasteurization	60-150
	Sterilization	100-140
	Distillation	40-100
	Blanching	60-90
	Scalding	50-90
	Concentration	60-80
	Tempering	40-80
	Smoking	20-80
Wood	Glueing	120-180
	Pressing	120-170
	Drying	40-50
	Steaming	70-100
	Cocking	80-90
	Staining	50-80
	Pickling	40-70
Plastic	Injection modling	90-300
	Pellets drying	40-150
	Preheating	50-70

Waste heat can be extracted from the heat source by different technologies presented in figure 10. These technologies are categorized into passive and active technologies is based on weather heat is directly utilized or converted to another form of energy or utilized at lower or higher temperature level. In passive technologies, heat is directly utilized, and dominant technologies are heat exchangers and thermal energy storage. In active technologies, heat is converted to another form of energy or temperature level is changed. These active technologies further divided into three types according to what these technologies generate. (Brückner et al, 2015)

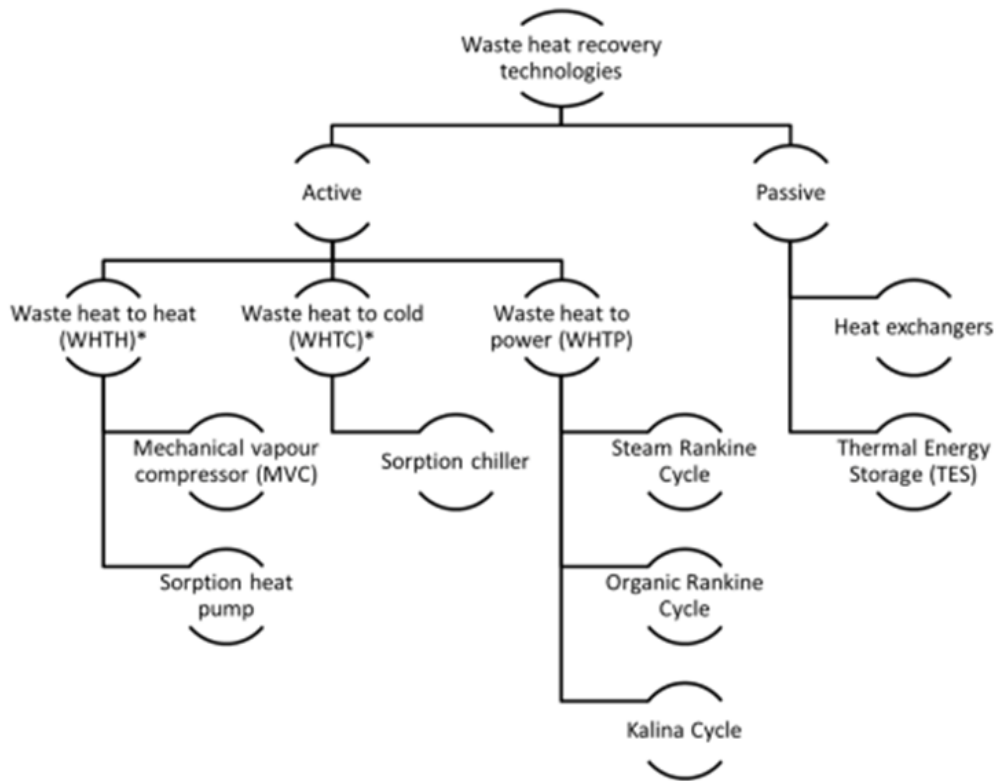


Figure 10. Categorization of waste heat recovery technologies (Brückner et al, 2015).

2.4.1 District heating network

District heating (DH) is commonly utilized heating method with market share of 45 % of space heating demand in Finland (Finnish energy, 2024). In general, DH is centralized heating system used in the urban areas. System comprises network of insulated pipes where hot water is distributed to customers of the distribution network. Heat is generated in centralized plants or in several individual heat production facilities. This flexibility of DH network enables utilization of many different heat sources and technologies. Size of DH network can range from a few houses all the way to entire city or region level. (Mazhar et al, 2018)

Figure 11 illustrates the development of different energy sources in Finnish DH production. Previously, fossil fuels have been dominating energy source for the DH production. However, share of fossil fuels have reduced during the last decades and biomass has become the main source for the DH production. Similarly, the share of heating methods based on electricity and waste heat has increased. Heat recovery and electricity in the figure 11 denotes to technologies such as waste heat, heat pumps and electric boilers (Finnish energy, 2024).

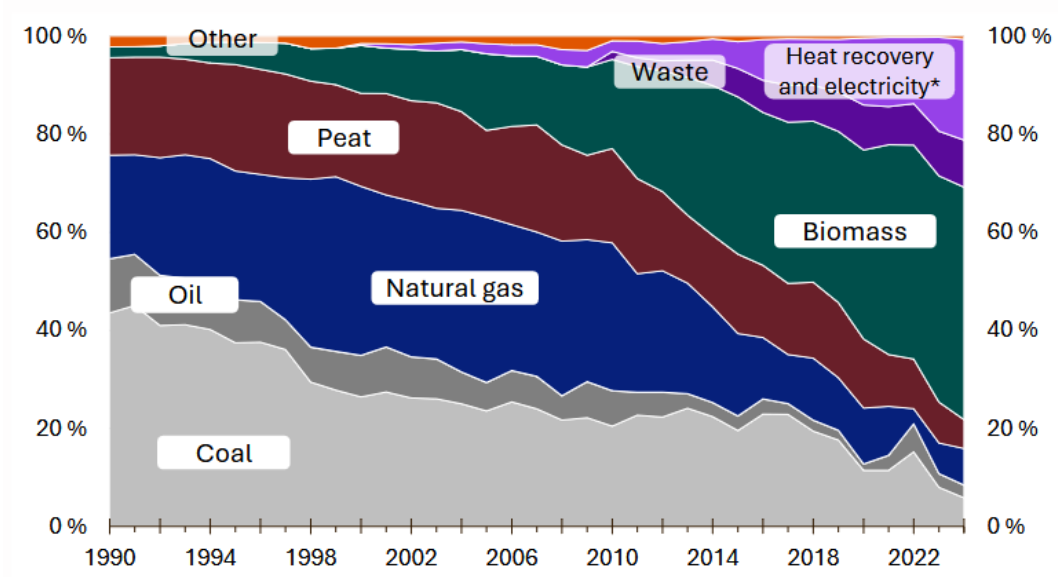


Figure 11. Energy sources of Finnish DH networks (Finnish energy, 2024).

Temperature of DH supply water varies depending on outside temperature. In Finland, DH water temperature in the supply pipe varies between 65 °C and 115 °C and in return pipe water temperature ranges from 40 °C to 60 °C. In addition, average heat losses of heat distribution network are between 8-9 %. (Finnish Energy DH Networks, 2024). DH networks can be categorized into different generation according to figure 12. Currently, third-generation DH is the applied generation in Scandinavian countries (Lund et al, 2021). Development trend of these district networks have been continuously towards to lower operating temperatures, increased energy efficiency and ability utilized more versatile mixture of different heat generation technologies. (Lund et al, 2021)

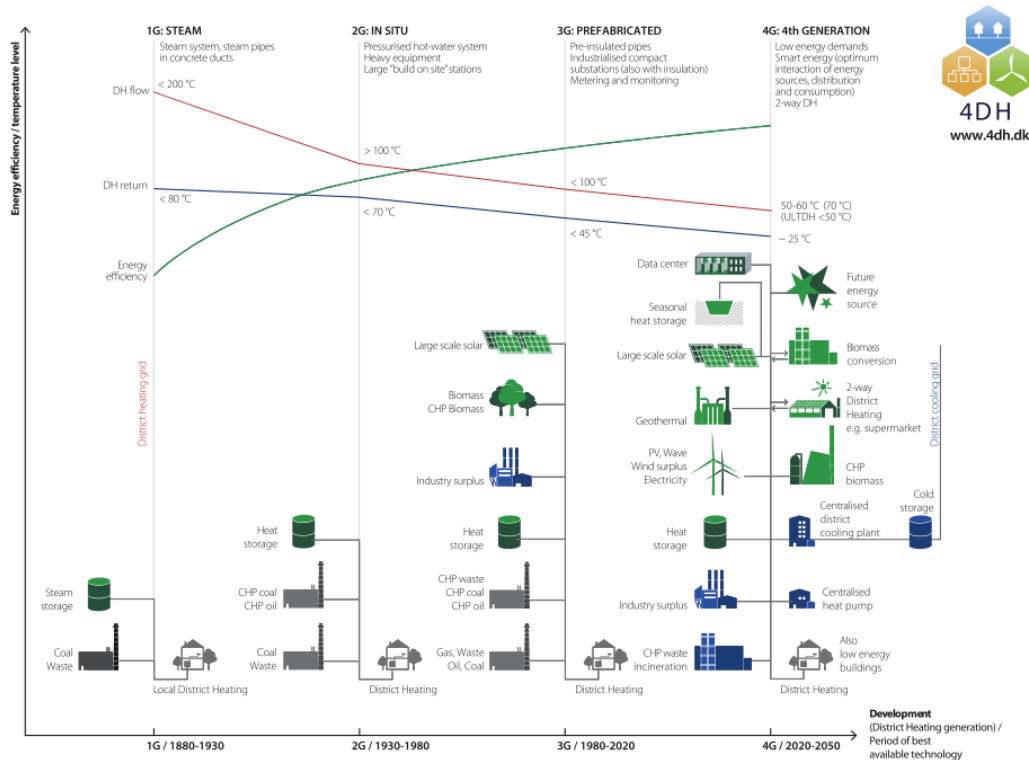


Figure 12. Illustration of DH network generations (Lund et al, 2021).

Next major development occurs when fourth-generation DH networks are implemented. In the fourth-generation networks, the lower operating temperature enables enhanced utilization of low temperature heat sources. Furthermore, low operating temperature could allow direct utilization of low temperature heat with heat exchangers without need for temperature boosting with heat pumps. Therefore, possibly improving the economic viability of low temperature heat sources since expensive heat pumps would not be needed anymore. Temperature levels of the fourth generation are typically high enough to fulfil space heating demand directly without need for temperature lift. (Lund et al, 2021)

The fourth generation is an interesting development direction from electrolyzer waste heat utilization perspective since AEL operating temperature is expected to increase in the future (David et al, 2019). In addition, high temperature AEL are recognized as efficient, scalable and low-cost alternative for green hydrogen production in the future. Operating temperature of high temperature AEL ranges from 100°C to 200°C that could enable direct utilization of waste heat on the supply side. (Lohmann-Richters et al, 2021) On the other hand, the waste heat from electrolyzer could be also used for preheating the return water (Meriläinen et al, 2024).

2.4.2 Industrial heat pumps

Purpose of industrial heat pumps is to raise temperature of low temperature level heat source to higher temperature level by using external heat energy source. Industrial heat pumps are also frequently called as high-temperature heat pumps due to high operating temperatures of the industrial heat pumps. These pumps can produce high temperature heat even over 90-100 °C (Kosmadakis, 2019). In addition, these electric driven heat pumps are suitable for flexible operating with minimum load of 20 % (Grosse et al, 2017).

In industry, a typical heat source is waste heat flow from a process that heat flow would be rejected without industrial heat pumps due to its low temperature (Kosmadakis, 2019). For efficiency of a heat pump cycle is termed to coefficient of performance (COP) which defined according to equation 20 where Q_{out} denotes to useful heat supplied from higher heat reservoir to system and P_{in} denotes to primary energy input into the cycle (Zhang et al, 2016).

$$COP = \frac{Q_{out}}{P_{in}} \quad (20)$$

For industrial applications, there are several different heat pumps cycles available on the market which can be divided into categories such as vapor compression cycle, mechanical, vapor recompression cycle, thermal vapor recompression cycle, absorption cycle, and chemical heat pumps (Zhang et al, 2016). Currently, the most common industrial heat pump technology is based on vapor compression cycle (Arpagaus et al, 2018). Figure 13 illustrates schematic diagram of most important components included in the vapor compression cycle and circulating direction of refrigerant through the entire closed cycle. Evaporator and condenser refer to heat exchangers in heat pump technology.

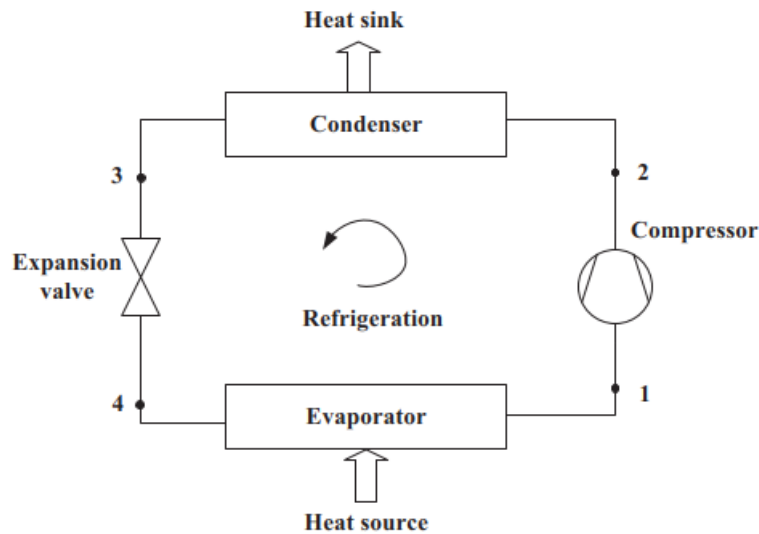


Figure 13 Schematic diagram of vapor compression cycle (Zhang et al, 2016).

Figure 14 presents the corresponding pressure-enthalpy diagram for ideal vapor compression cycle. The working principles of this cycle are following. In the evaporator, heat is absorbed from heat source to refrigerant. Then, the superheated refrigerant is compressed by compressor to state point 2. After that, the refrigerant flows to condenser where hot vapor is condensed, and heat is released to heat sink. In the condenser, refrigerant goes through phase change from vapor to liquid. At final part of the cycle, refrigerant flows through the expansion valve where temperature and pressure of refrigerant are reduced to back to state point 4 level, hence completing the cycle.

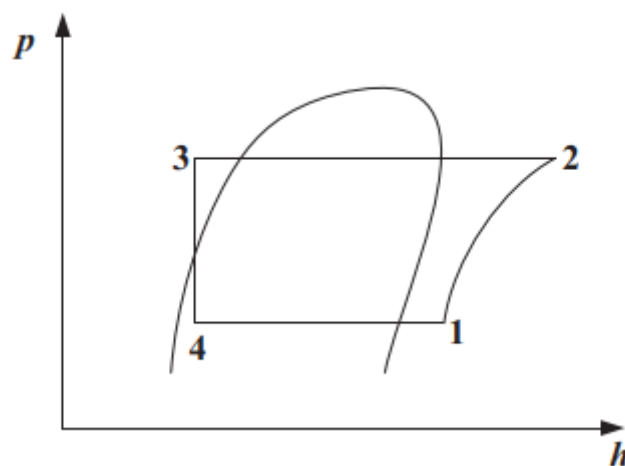


Figure 14 Pressure-enthalpy diagram of ideal vapor compression cycle (Zhang et al, 2016).

The selection of suitable refrigerant is important aspect since the properties of refrigerant effect on many factors such as thermal suitability, safety, efficiency, availability and environmental compatibility (Arpagaus et al, 2018). The refrigerant should be selected hence that there is at least 10 K to 15 K temperature difference between desired condensation temperature and critical point of refrigerant in order ensure proper heating COP value (Arpagaus et al, 2018). Compressor isentropic efficiency of industrial heat pumps varies usually between 0,7-0,8 (Arpagaus et al, 2018).

Table 4 presents properties of refrigerants commonly utilized in high temperature heat pump applications where ODP denotes to ozone depletion potential, GWP to global warming potential for 100-year time horizon and SG to safety ground classification that relates toxicity and flammability of a refrigerant. R134a and R245fa are presented as reference refrigerants which have been most utilized refrigerants recently in large-scale electric heat pumps in DH systems (David et, 2017). However, these high GWP potential refrigerants are expected to be phase out and replaced by low GWP potential alternatives such as R1234ze(E), R1234ze(Z), R1336mzz(Z) and R1234yf (Arpagaus et al, 2018). In addition, according to survey of David et, 2017 natural refrigerants such as ammonia and carbon dioxide are applied in heat pumps in DH systems. Disadvantage of these natural refrigerants is the need for high operating pressure.

Table 4 Properties of refrigerants for industrial vapor compression heat pumps (Arpagaus et al, 2018, Zhang et al, 2016 & Hu et al, 2017).

Refrigerant	Critical temperature (°C)	Critical pressure (bar)	ODP	GWP	SG
R134a	101,1	40,6	0	1300	A1
R245fa	154,0	36,5	0	950	B1
R1234ze(E)	119,45	36,4	0	6	A2L
R1234ze(Z)	150,1	35,3	0	2,2	A2L
R1234yf	94,7	33,8	0	4	A2L
R1336mzz(Z)	171,3	29	0	2	A1
NH ₃	132,3	113,3	0	0	B2
CO ₂	31,1	73,8	0	1	A1

With large temperature lifts and higher temperature outputs multi-stage heat pumps are utilized to achieve higher COP value since single-stage heat pumps exergy losses are high in the compression and expansion process. Hence, lowering the single-stage heat pumps performance. In multi-stage heat pump, compression of refrigerant occurs in multiple compressors. Therefore, enabling achieving higher compression evaporator temperatures with higher compression efficiency. Otherwise, working principles and components of

multi-stage heat pumps are same as one stage heat pumps presented figures 15. (Hu et al, 2017)

2.4.3 Organic Rankine cycle

Organic Rankine cycle (ORC) is thermodynamic cycle used to convert heat to electric power. This conversion cycle is applied usually with low temperature and medium heat sources such as waste heat, biomass combustion and geothermal heat. (Pethurajan et al, 2018) In the ORC, heat source temperature can vary from 80 °C up to 500 °C (Bao & Zhao, 2013). Similarly, useful power of the cycle can vary from few kW up tens of MW (Rahbar et al, 2017).

From the system layout perspective ORC and steam Rankine cycle are similar. Only difference between these cycles is in unitized working fluids. Steam Rankine cycle utilizes water as working fluid when ORC utilized various organic fluids. (Pethurajan et al, 2018) However, organic fluids have lower critical pressure and temperature than water. Therefore, organic fluids can be applied with various low- and medium type heat sources. High molecular weight of organic fluids enables better turbine efficiency with same sized system due to higher mass flow rate. (Pezzuolo et al, 2016) Furthermore, ORC can maintain higher partial load efficiency than steam turbines of Rankine cycle and ORC can maintain stable operation at 10–15% of its nominal load (Witkowski et al, 2020).

Figure 15 illustrates system layout and working principles of the simplest ORC configuration. The cycle consists of four main components such as a pump, a condenser, an expander and an evaporator. Process working principles of process are following. Pressure of liquid working fluid is increased by the pump (1-2). Then, working fluids heat sources in the evaporator forming high temperature and high-pressure vapor (2-3). Next high-pressure vapor flows into expander where thermal energy of working fluid is converted into mechanical energy of rotating turbine blades which is then converted to electric power by generator (3-4). Finally, working fluid flows into condenser where it is cooled by external cooling source to initial conditions hence completing the cycle (4-1). (Jiménez-García et al, 2023)

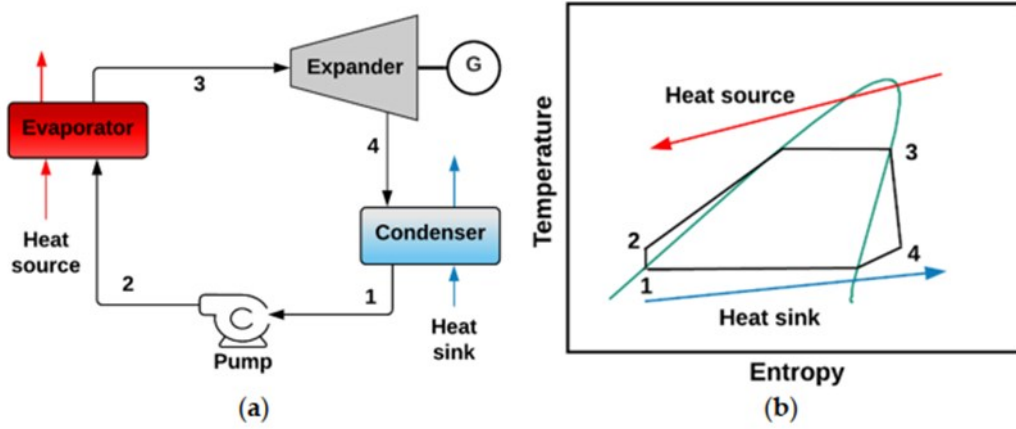


Figure 15. Basic ORC (a) Schematic diagram (b) T-s diagram of the cycle (Jiménez-García et al, 2023).

Thermal efficiency of thermodynamic cycle can be determined according to the equation 21 where W_{net} refers to the net work output of the system that is calculated as difference between work of turbine $W_{turbine}$ and pump work W_{pump} while Q_{in} denotes the thermal energy supplied into the cycle. (Jiménez-García et al, 2023) Typical method to improve ORC efficiency is to add internal heat exchanger between the turbine outlet and condenser inlet. Purpose of this recuperative heat exchanger is to preheat the input working fluid before evaporator. Then, reducing the heat supplied by the evaporator. (Pethurajan et al, 2018)

$$n_t = \frac{W_{net}}{\sum Q_{in}} = \frac{\sum W_{turbine} - \sum W_{pump}}{\sum Q_{in}} \quad (21)$$

Selection of suitable working fluid for ORC is an important aspect to obtain high thermal efficiency and maximize heat extraction from the heat source. There are lot of thermo-physical properties influence on selection of suitable working fluid. However, to achieve good efficiency a fluid should be selected so that critical temperature is close to maximum temperature of the heat source. Furthermore, selection of fluid influences other aspects such as system stability, safety, economic viability, components size and environmental impact. (Rahbar et al, 2017) The heat source of this thesis can be categorized as a high temperature heat source in the context of ORC. Hence, literature recommends following working fluids such as benzene, toluene and cyclohexane based on heat source temperature and critical temperature of fluids (Rahbar et al, 2017). Table 5 presents information of selected suitable working fluids for ORC and water is presented as reference working fluid utilized in steam Rankine cycle.

Table 5. Critical conditions and molar masses of selected working fluids (Nguyen et al, 2010).

Fluid	Molar mass (g/mol)	Critical temperature (°C)	Critical pressure (bar)
Water	18.02	374,2	221,18
Benzene	78,11	288,9	48,95
Toluene	92,14	318,64	41,08
Cyclohexane	84,16	280,39	40,73

In the reality, there are practical restrictions for evaporator and condenser pressure to ensure system stability. Table 6 illustrates the practical limits of the ORC for selected working fluids. Maximum evaporator pressure is determined way that presence of liquid is avoided in any part of the turbine. Condenser pressure is calculated based on assumption that minimum condensation temperature is set to 25 °C or condenser is set to minimum pressure of 0,05 bar which is the lowest pressure that can be applied (Rayegan & Tao, 2011)

Table 6 Practical limits of the ORC for selected fluids (Rayegan & Tao, 2011).

Fluid	Maximum P_{eva} (bar)	Maximum T_{eva} (°C)	Minimum P_{con} (bar)	Minimum T_{con} (°C)
Benzene	40,67	274	0,127	25
Toluene	35,76	307	0,051	31
Cyclohexane	36,65	272	0,13	25

3 Green ammonia plant model

The model for green ammonia plant is created in Aspen Plus software containing of an AEL, a heat pump, a Haber Bosch ammonia synthesis, ORC and Rankine cycle. Physical method applied in all components except the AEL and Rankine cycle is Peng Robinson. In the AEL model utilized physical method is ELECNRTL that is suitable method with electrolyte applications according to the Aspen Plus method assistant. In Rankine cycle, selected method is IAPWS-95.

Thermal losses out of the components are ignored in this model. Similarly, degradation of all components is ignored. Cryogenic air separation unit is not included in the model since it is not generating much waste heat. Furthermore, hydrogen storage is also not included in the Aspen Plus model since storage cannot be modelled with steady state software utilized in this thesis.

3.1 Alkaline electrolyzer model

The full-scale AEL electrolyzer plant modelled consists of 30 stack each with 10 MW electric power and all connected in parallel. Thus, resulting maximum electric power of the plant is 300 MW. However, due to convergence issues associated with design specks in the full-scale system only a single stack is modelled in Aspen Plus. The electrolyzer model is developed using data collected from literature, manufacturer websites and Aspen Plus. Table 7 illustrates key technical details of the electrolyzer model. Mass balance of single AEL stack is presented in table 8 and the flowsheet of whole model is presented in figure 18.

The number of cells per stack is iteratively adjusted in Aspen Plus to achieve the desired current density. The stack is simulated as isothermal with an external cooling cycle utilized to extract waste heat purely from the stack. The incoming feed stream is heated to operating temperature of the stack before entering the stack. Furthermore, rigorous option of Aspen Plus model is utilized and a setting correlation that includes the liquid head is selected for the pressure drop calculation inside the stack. The rigorous model requires geometry values as input. Default values of geometry for industrial scale electrolyzer are utilized except the cell area is modified to get proper current density.

Table 7. Technical specifications of single AEL electrolyzer stack model.

Specifications at nominal power		Unit	Reference
Stack power	10,0	MW	Sunfire, 2024
KOH	26,0	W%	Sunfire, 2024
Number of cells per stack	382,0		Iteration result
Current density	4128	A/m ²	Aspen Plus result
Cell voltage	2,11	V	Aspen Plus result
Cell area	3,0	m ²	Buttler & Spliethoff, 2018
Operating temperature	70,0	°C	Buttler & Spliethoff, 2018
Pressure	30,0	bar	Sunfire, 2024
Pump isentropic efficiency	70,0	%	Aspen Plus examples library
Demi water consumption	1590,4	kg/h	Aspen Plus result
Total circulating stream inside Stack	100	kg/s	Own assumption
Pure hydrogen production	175,1	kg/h	Aspen Plus result
Feed stream split fraction between anode and cathode	25,0	%	Aspen Plus examples library

Table 8. Mass balance of single AEL stack.

	H2O-IN	O2-OUT	COND	Pure H2	Unit
Temperature	20,0	70,0	70,0	382,8	°C
Pressure	1,0	29,8	29,8	200,0	bar
Mass vapor Fraction	0	1	0	1	-
Mass Flows	1590	1404	12	175	kg/hr
H2O	1590	7	12	0	kg/hr
H2	0	1	0	175	kg/hr
O2	0	1396	0	0	kg/hr

The layout of the AEL model is partly based on example model found from the Aspen Plus example library. Mass balance of the electrolyzer is maintained in balance by a calculator in the Aspen Plus when power of electrolyzer is varied. The calculator determines the required feed water mass based on the mass outputs from the electrolyzer system. In addition, the electrolyzer model includes hydrogen purification and compression on the cathode side.

3.2 Haber-Bosch model

The Haber-Bosch model is developed based on Lin et al, 2020 and Araújo, A. and Skogestad, S, 2008 papers of the simplified design of Haber-Bosch process with Aspen Plus. This simplified model illustrates typical conventional high-pressure reaction-condensation Haber-Bosch process. Process is fed by pressurised pure hydrogen and nitrogen. Therefore, purge can be ignored in this model. Amount of nitrogen fed to Haber-Bosch process is calculated from stoichiometry of the ammonia synthesis reaction using the Aspen Plus calculator tool where molar flow of hydrogen is a known parameter. Figure 16 presents the flowsheet of the developed Haber-Bosch model. Table 9 presents the mass balance the key input and output flows of Haber-Bosch model.

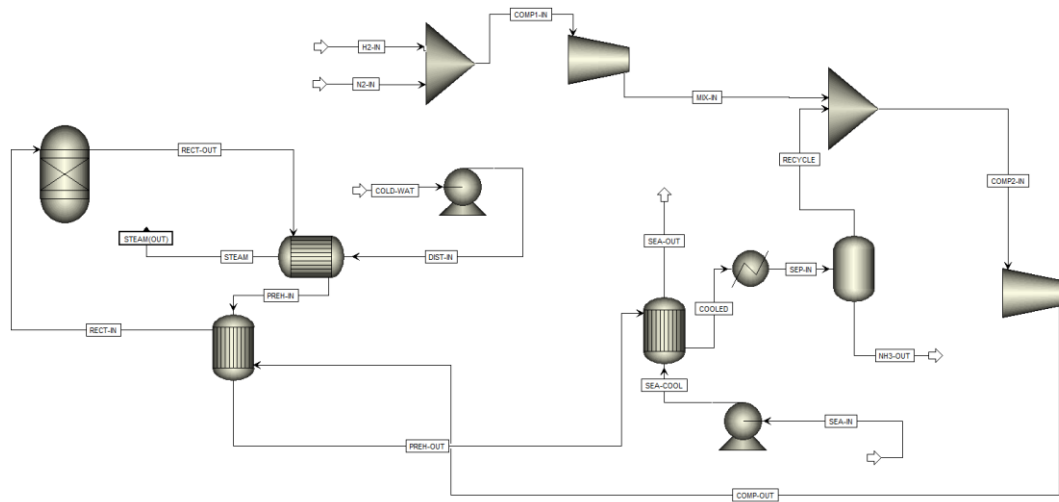


Figure 16. Flowsheet of Haber-Bosch model.

Reactor is modelled as an isothermal RGibbs reactor and model includes only one preheater before the reactor. The waste heat generated by ammonia synthesis is extracted from outlet stream of the reactor by heat exchanger. This extracted high pressure and temperature heat steam is then utilized in the scenarios of this thesis. Due to heat integration of Haber-Bosch process part of heat must be utilized to preheating input stream into the reactor. Otherwise, working principle and components of the model same as in figure 5.

Table 9. Mass balance of Haber-Bosch model.

	COLD-WAT	H2-IN	N2-IN	NH3-OUT	STEAM	Unit
Temperature	40	20	20	-33	250	°C
Pressure	10	30	30	196	40	bar
Mass Vapor Fraction	0	1	1	0	1	
Mass Flows	30080	5253	24331	29583	30080	kg/hr
H2O	30080	0	0	0	30080	kg/hr
H2	0	5253	0	13	0	kg/hr
N2	0	0	24331	59	0	kg/hr
NH3	0	0	0	29511	0	kg/hr

This Haber-Bosch model operating pressure is set to 200 bar and the reactor outlet temperature is 498 °C with single pass ammonia conversion of 29,6 %. The inflow stream to the reactor is preheated to 235 °C utilizing heat recovered from the outflow stream of the reactor. Furthermore, ammonia separation is very simplified since ammonia separated by firstly cooling the stream to -33 °C. Then, liquid ammonia separated from unreacted hydrogen and nitrogen by a flash. Resulting ammonia purity of 95,5 mol%.

3.3 Electricity generation model

Electricity generation model is separate closed cycle in the Haber-Bosch model which utilizes the high temperature and pressure waste heat generated in ammonia synthesis occurring in the RGibbs reactor. Configuration of electricity generation model is simple ORC and the flowsheet the model is presented in figure 17. Turbine efficiencies inputs are following mechanical efficiency 99 % and isentropic efficiency 85 %. Pump isentropic efficiency is set to 70 %. (Karellas et al, 2013) In addition, the model contains two design specks. Purpose of the first design specks is to adjust the mass flow inside the ORC with target to Haber-Bosch stream outlet temperature of 250 °C in order have enough heating power for preheating before the RGibbs reactor. The second design speck adjust cooling water mass flow through condenser with target that cooling water temperature increase is equal to 2,8 °C. Utilized specifications with different working fluids are presented in the appendix.

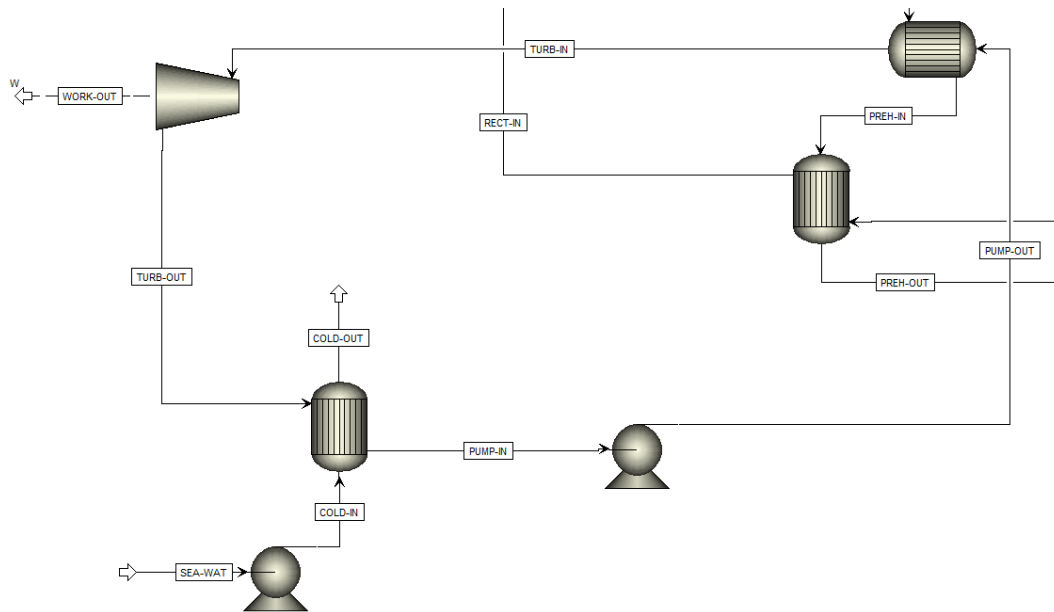


Figure 17. Flowsheet of the electricity generation model.

3.4 Heat Pump model

Heat pump model developed for this thesis is one stage pump with vapor cycle. The model consists same components as presented in the figure 13 in the literature review part. All heat supplied for the evaporator comes purely from the stack and the model is created to illustrate cooling cycle where refrigerant flows through the stack. R1234ze(E) hydrofluoroolefin is selected to refrigerant due to this refrigerant suitable for properties perspective for the desired condenser temperature. Furthermore, this hydrofluoroolefin has low GWP value and good SG classification. Compressor isentropic efficiency is set to 80 %.

The model contains the design specs which are utilized to calculate different operating conditions such as supply temperature and waste heat generation. The first design specs adjust the mass flow of the refrigerant inside heat pump system with target to superheat refrigerant by 5 °C at evaporator. The second design spec adjust the mass flow DH water through the condenser with target to heat DH to required temperature. Incoming water for the evaporator assumed be a constant 40 °C and leaving supply water temperature from evaporator is changed according to the temperature needed in the DH. The heat pump is separated from electrolyzer due to convergence errors related to design specs when heat exchanger is directly connected to input stream of the stack.

4 Research material and methods

This chapter describes the material and methods used as input data to parametric simulation of DH production for year 2024. The simulation is conducted for two cities of differing sizes, Kokkola and Oulu. Cities are located on the west coast of Finland, on the shores of the Gulf of Bothnia. These locations were chosen since they are potential alternatives for a green ammonia plant in Finland. Furthermore, this chapter presents the assumptions used in the calculation of the levelized cost of DH based on parametric simulation results. All data used in this thesis is collected from sources at the hourly level. Hence, the simulation is also conducted at the hourly level.

4.1 Input data

Data utilized in this thesis is collected from open sources except the hourly districting consumption data provided by Oulu Energia and Kokkola Energia. This hourly-level consumption data is considered confidential. Therefore, it cannot be presented in this thesis. This data is utilized on for sizing of the heat pump system and calculating the number of hours during which heat pump production could exceed the DH network demand. The DH consumption data do not include losses of DH-network.

All weather data is taken from Finnish meteorological institute data base that is based on real measurements (Finnish Meteorological Institute). For the outside temperature, Kaukovainio observation station was selected which is located near the city centre. In Kokkola, Santahaka observation station was selected with similar location respect to the city centre as in Oulu. Sea water temperature is taken from an observation buoy located at bay of Bothnia. This buoy was the only observation site which included full year measurements of entire year of bay of Bothnia. The average seawater temperature is used to represent the cooling water temperature in both the Haber-Bosch process and the ORC. Figure 19 illustrates the utilized DH network supply water temperature profile. The upper boundary of the red shaded area is used in this thesis since according to Oulu Energia the maximum supply water temperature currently is 115 °C in Oulu.

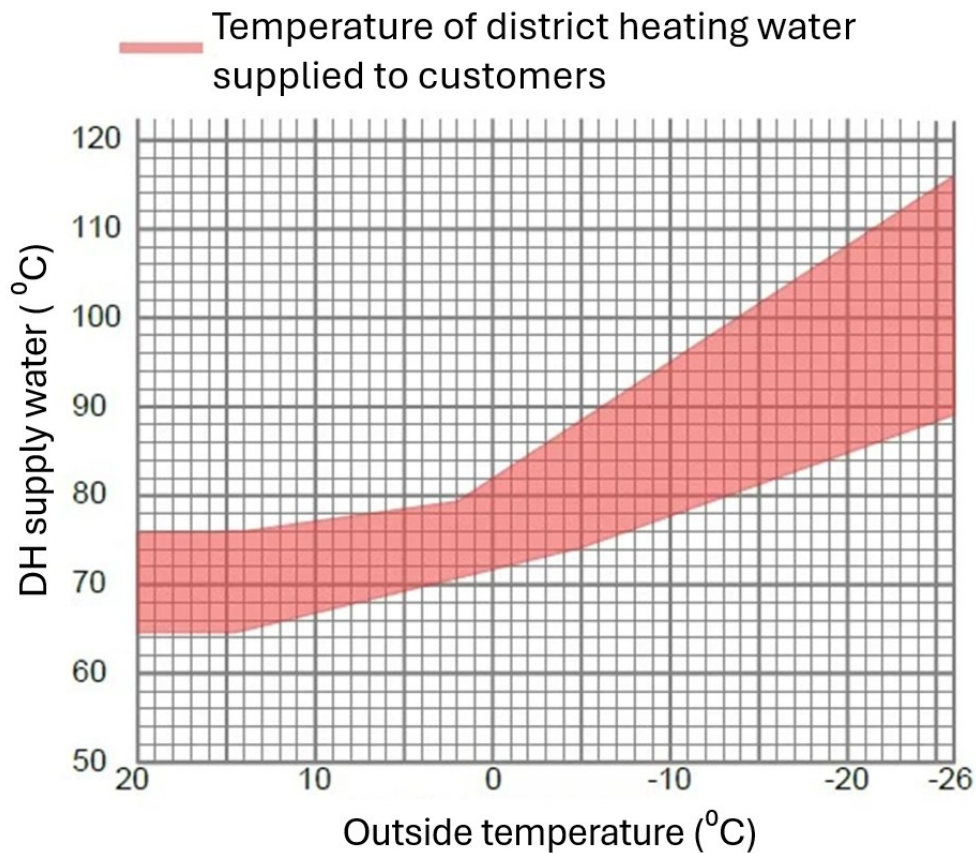


Figure 19. Supply side water temperature of DH network modified from (Helen).

Renewable power generation is simulated with Renewables.ninja which is open-source online tool that can be used simulate wind power and solar photovoltaic power based on weather data from global reanalysis models and satellite observations (Renewables.ninja). The weather data utilized is NASA MERRA 2 for both technologies. The selected wind turbine model is the Siemens Gamesa SG 6.6-170 with hub height of 150 m. The photovoltaic (PV) panels are south facing with tilt angle of 40°.

Chosen locations of wind farm and solar farms are given in figure 20 where blue icons illustrate wind power and yellow ones illustrate solar power. The locations of farms are selected based on real location of the farms under development or recently constructed (Renewables Finland). The wind turbine model is selected from recently completed onshore-wind farm project (OX2). The modelled renewable power generation includes three wind farms and two solar farms with an installed capacity ratio of wind to solar energy of 3:1. The farms are geographically distributed across of Finland to better illustrate real renewable power supply for a green ammonia plant.

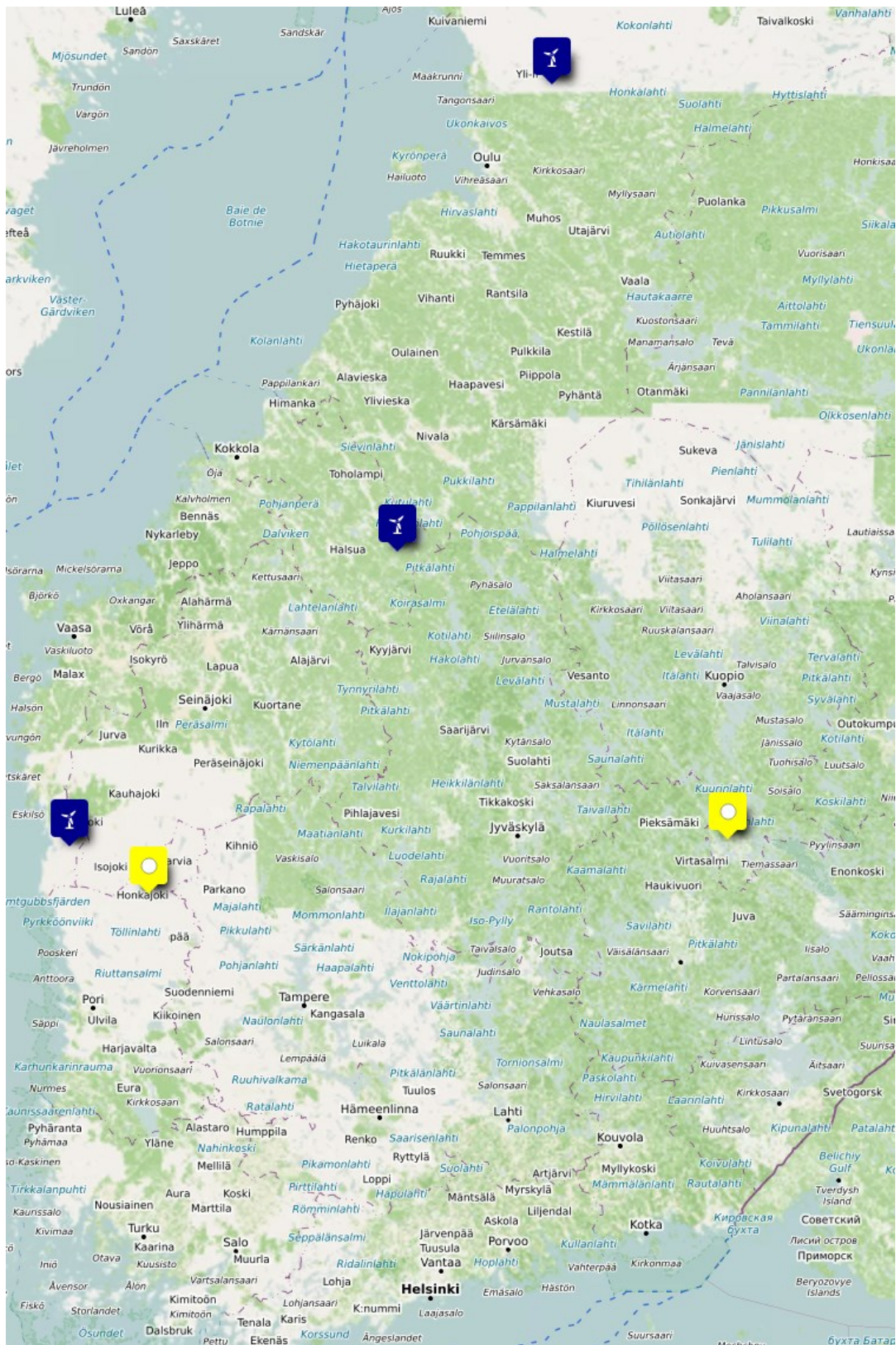


Figure 20. Locations of wind farms and solar farms used in Renewables.ninja.

4.2 Parametric calculations

The aim of the parametric calculations is to simulate industrial scale green ammonia plant with annual production over 200 kt/NH₃. The focus on the calculation is to simulate DH production from waste heat generation of the plant. Firstly, Aspen Plus model presented in the figure 18 is utilized to calculate waste heat generation and electricity consumption of DH production with different AEL power levels and DH supply temperature values. In second phase, MATLAB code is created where parametric results from Aspen Plus are combined with input discussed in previous in chapter. Ramping constraints of all components of model are neglected as engineering simplification. Secondly, the behaviour of key parameters during the ramping stage is unknown since Aspen Plus is a steady-state simulation program. Possible electricity grid restrictions are ignored. Therefore, the plant production profile and theoretical waste heat generation can be assumed to be the same in both cities.

4.2.1 Aspen Plus

In the Aspen Plus simulations, calculations principles differ between low- and high temperature cases. For scenarios with low DH supply temperatures, results such as heat pump electricity consumption, waste heat generation, DH production, and pure hydrogen output are collected using the sensitivity analysis tool. The parameter varied in the sensitivity analysis tool is the power supply into single stack is varied from 2 MW to 10 MW with 1 MW increment. This simulation is repeated with following DH supply temperature levels 70 °C, 80 °C and 90 °C.

In the high temperature cases, hydrogen feed rate into Haber-Bosch process and DH supply temperature are the parameters varied. Maximum hydrogen feed rate is defined to 5252,6 kg/h corresponding to maximum hydrogen production capacity of all AEL stacks. The feed rate is varied at 100 %, 90 %, 75 %, 50 %, and 20 % of this maximum value. The DH supply temperature targets for all feed rates are 100 °C and 115 °C.

Equation 22 illustrates the principle used to calculate total DH production in the high temperature cases. In this equation, n_{stack} denotes the number of stacks connected to DH production, Q_{HP} represents heat pump heat generation and Q_{HB} denotes to heat exchanger heat duty after mass multiplier tool shown in figure 18. The last two variables in the equation 22 are illustrating the heat from single stack connected to district production.

$$Q_{total} = n_{stack}(Q_{HP} + Q_{HB}) \quad (22)$$

The calculating principle is following. Firstly, Q_{HB} is calculated with all different hydrogen feed rates and target temperatures. Then, theoretical DH total production with all scenarios is calculated by increasing number of stacks. Q_{stack} values are known from low temperature cases with target temperature of 90 °C. However, not all combinations of target temperature and hydrogen feed rate can achieve higher temperature targets. Therefore, the limits are checked in Aspen Plus. This is check by increasing the number of stacks until the supply water can no longer be heated to the desired target temperature. This limitation indicates a violation of the minimum temperature approach in the heat exchanger or crossing of the heat curves. Beyond the limit, target temperature cannot be reached by increasing if number of stacks is increased. For the high-temperature cases, the electricity consumption of the circulation pump related to steam production is collected from the Aspen Plus model for all hydrogen feed rates. In scenarios where steam is not fully utilized to heating supply water, the unused portion is assumed to be lost as waste.

4.2.2 Programming

The green ammonia plant is assumed be powered by a power purchase agreement (PPA) which includes 70 MW of baseload and the rest of PPA is pay-as produced PPAs. Renewable power generation data discussed earlier corresponds to the pay-as produced part of the PPA. The baseload is utilized ensure continuity operations of the AEL and Haber-Bosch process and avoid unwanted degradation of the AEL. Therefore, control strategy of stack is that every stack is operated with same power level all the time and stacks are always on. The only exception is the 20-day maintenance break scheduled to begin on July 1st. During the maintenance break the whole green ammonia plant is fully shutdown. The PPA exclusively supplies power to the AEL and the Haber-Bosch process. DH production related components such the heat pump system and pump associated to steam production are powered by spot priced electricity.

The code begins by calculation of daily DH supply temperature values based on corresponding outside temperature values and logic behind temperature limits is presented in appendix. DH supply temperature is calculated by averaging the outside temperature values of each day. This daily average is then utilized to determine a constant DH supply temperature for the entire day.

Next, operation of the AEL is simulated using input data including PPA power and DH supply water temperature. The power of green ammonia plant is adjusted according to availability of renewable power. The code determines the maximum integer electric power supplied into AEL. Based on this, hydrogen production is calculated by utilizing data obtained from the Aspen

Plus model. Hydrogen production is calculated as the product of the number of operational stacks and hydrogen output per single stack for given power level of stack. In this simulation, number of stacks operational is always 30 due to control strategy of stacks.

The hydrogen storage simulation is carried by utilizing mass balance equation 23. Capacity of the storage is 20,000 kg of hydrogen, and it is initially assumed to be half full. In equation 23, consumption describes the feed rate of hydrogen into Haber-Bosch process. To avoid continuous ramping of the Haber-Bosch process and reduce high fluctuations in storage level caused by small storage capacity. The process feed rate is kept as constant for every four hours.

$$m_{h_2}(t + 1) = m_{h_2}(t) + m_{h_2}(t)_{production} - m_{h_2}(t)_{consumption} \quad (23)$$

The simulated plant production is iterated to correspond industrial scale green ammonia plant annual ammonia and hydrogen production values by varying the maximum power of pay-as produced PPA. This approach ensures creation of a realistic production profile for the plant. Annual ammonia production is calculated based on data obtained Aspen Plus model by matching simulated hydrogen feed rate into Haber-Bosch process to corresponding ammonia production value.

By applying calculating parameters such as stack power, hydrogen feed rate into Haber-Bosch and DH supply temperature are used to calculate the DH production and electricity consumption production profiles. Calculating principles for both are similar that code matches corresponding value for DH production or electricity consumption from Aspen Plus dataset according to the specified calculating parameters. Then, dataset value is multiplied by the number of stacks connected to DH production. Equation 24 illustrates equation utilized to calculate electricity consumption of DH production where P_{HP} is single heat pump electricity consumption and P_{HB} denotes the pump utilized steam generation in Haber-Bosch model. DH production is calculated similar way as in equation 22. In low temperature cases, Q_{HB} and P_{HB} are equal to zero.

$$P_{DH} = n_{stack} P_{HP} + P_{HB} \quad (24)$$

Sizing of heat pump systems is conducted by iterating the number active stack connected to DH production. Then, comparing the iteration results against the DH consumption data. Objective function of this iteration is to minimize annual number of hours during which DH production exceeds the DH network demand during the operational hours of the green ammonia plant.

There are two special situations in the simulations code. During periods of DH overproduction, the number of stacks connected to DH production is curtailed until DH production no longer exceed the DH network demand. In the second special scenario, when DH supply water cannot be heated to desired target temperature under high temperature scenarios. Those hours are simulated as low temperature case with DH supply temperature of 90 °C. Thus, the steam is not utilized to heat DH water. This simplification is done to reduce number of different scenarios in the model and reveal limits for suitable heat pump size. Number of hours under both special scenarios is counted and presented in the results.

4.3 Levelized cost modelling

Based on parametric simulation results economic feasibility of produced DH is evaluated by levelized cost of heat (LCOH) which is calculated by dividing the discounted lifetime investment cost by the discounted lifetime heat production. Equation for LCOH is presented in equation 24 where CAPEX refers to total capital expenditure, OPEX denotes to annual operational expenditure, $E_{h,t}$ is the annual DH production, t is time in years, n refers to expected lifetime of investment, r is the discount rate and $E_{h,t}$ is the annual DH production (Ebenhoch et al, 2015).

$$LCOH = \frac{CAPEX + \sum_{t=1}^n \frac{OPEX}{(1+r)^t}}{\sum_{t=1}^n \frac{E_{h,t}}{(1+r)^t}} \quad (24)$$

Table 10 presents assumption used in LCOH calculations. All cost presented in this thesis are exclusive of value added tax. The green ammonia plant is connected to the Fingrid transmission network. The variable consumption fees listed in the OPEX section of table 10 correspond to electricity transmission costs. In addition, DH production with heat pumps is eligible to lower electricity tax category in Finland (Vero). Electricity tax includes the supply of the security fee for electricity.

Table 10. Assumptions of LCOH calculations.

Parameter	Unit	Value	Reference
Discount rate	%	2,4,6,8,10,12	Own as- sumption
Lifetime	years	20	Grosse et al, 2017
Operational days annually	days	346	Green North Energy Oy. (2023)
OPEX			
Electricity tax category	€/MWh _{el}	0,63	Vero
Electricity price	€/MWh	Hourly spot Fin- land 2024	ENTSO-E
Output from the grid	€/MWh _{el}	0,99	Fingrid
Consumption fee winter months 7am to 9am	€/MWh _{el}	9,69	Fingrid
Consumption fee other times	€/MWh _{el}	2,75	Fingrid
Heat pump (variable)	€/MWh _{th}	1,75	Grosse et al, 2017
Heat pump (fixed)	€/MW/a	2850	Grosse et al, 2017
Haber-Bosch DH com- ponents	€/a	300 000	Own as- sumption
CAPEX			
Heat pump	M€/MWh _{th}	$(0,352 * Q_{hp}^{-0,122})^2$	Meriläinen et al, 2024
Haber-Bosch DH com- ponents	€	3 000 000	Own as- sumption
DH pipeline construc- tion cost	€/m	637	Finnish En- ergy statistics (2024)
Desing of new DH pipe- line	%	10	Own as- sumption 10% of con- struction cost

On the CAPEX side, it is assumed that 5 km of new DH pipeline will be constructed. The estimated construction cost is based on a pipe size of DN 300–400. Heat pump CAPEX illustrates the single heat pump specific investment cost for 1-10 MW_{th} and the Q_{hp} denotes to heating capacity of a heat pump (Meriläinen et al, 2024). Typically, a large heat pump systems comprise multiple units connected parallel. In this thesis, every heat pump is assumed have

same heating capacity. No relevant source was found for Haber-Bosch side components associated to DH production. Therefore, the cost of the pump and waste heat recovery boiler are estimated according to table 10.

5 Results and discussion

This chapter presents results in relation to model validation, parametric simulations, and LCOH calculations for a green ammonia production plant. Therefore, focus of this chapter is to answers to research questions 3,4 and 5. In the literature review part it was discovered that there are lot of industries and processes that can potentially utilized waste heat of green ammonia plant. Green houses and DH networks were identified most attractive application for the waste heat utilization. However, existing green houses are located on countryside far away from green ammonia plants which are planned constructed next to deepwater ports. This distance separation reduces feasibility of heat utilization in greenhouses compared to DH networks which are typically closer to ports.

5.1 Model validation

Comparison of simulated and measured experimental polarization curves is common method utilized to validate an electrolyzer stack. Figure 21 presents the comparison of polarization curves between simulated model and experimental data. Stack is operating conditions of the comparison are following 75 °C and 7 bar. In addition, stack consist of 12 cells with active area of 0,1 m² and concentration of potassium hydroxide in water is set to 35 w%. In this chapter, all simulation data from Aspen Plus is collected using the sensitivity analysis tool.

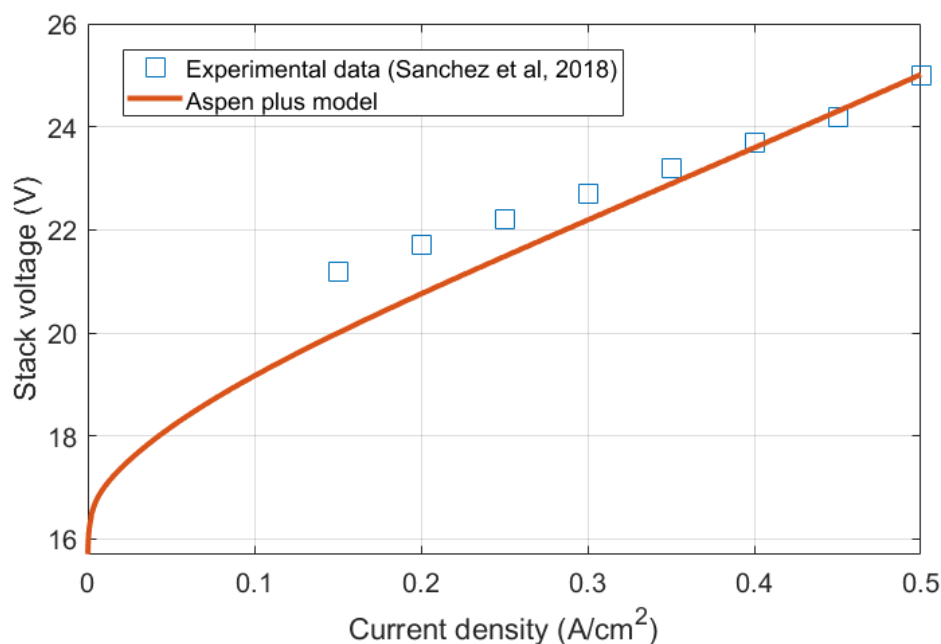


Figure 21. Comparison between experimental data and Aspen plus model polarization curves of the AEL.

In the simulated model, default specifications of industrial scale Aspen Plus stack model are used expect for the active area and the number of stacks. These specification values are not public material, and experimental data is taken from small scale stack. Therefore, the model results differ from experimental results. Nevertheless, the results of figure 21 demonstrates that polarization curve of the model is reasonable.

Validation of the electrolyzer model waste heat generation from the stacks is conducted with full scale model of this thesis. The results of validation presented in the figure 22 that illustrates part of the input power is correctly converted into waste heat in the Aspen Plus stack model. The theoretical heat generation is calculated from equation 25 where HHV denotes higher heating value of hydrogen, m_{h_2} indicates the known hydrogen production from the stacks and P_{el} refers to electric power supplied into stacks. Equation 25 is based on efficiency equation 12 introduced earlier in this thesis. The AEL stacks are operated as isothermal at constant temperature of 70 °C and pressure of 30 bar. Load flexibility of the stacks is assumed be range from 20 % to 100 %.

$$Q_{theo} = \left(1 - \frac{m_{h_2} HHV}{P_{el}}\right) P_{el} = P_{el} - m_{h_2} HHV \quad (25)$$

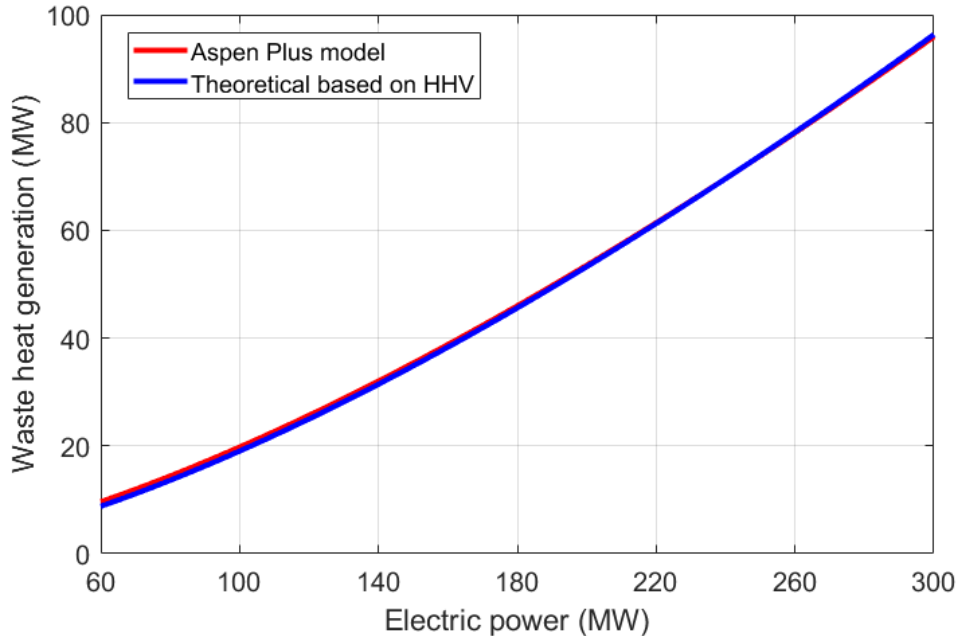


Figure 22. Validation of the electrolyzer model waste heat generation.

Haber-Bosch process validation is completed by validation of isothermal GIBBS reactor ammonia content in equilibrium with stoichiometric reaction ratio of pure hydrogen and nitrogen. The model results are compared to literature data of Appl, 2021. This literature data is based on the analytical expression of the equilibrium constant developed by Gillespie and Beattie, 1930 and the data is calculated utilizing their equations. Figure 23 illustrates ammonia conversion as a function of temperature with three different pressure levels. It can be observed from figure 23 that there is clear correlation between model results and literature data.

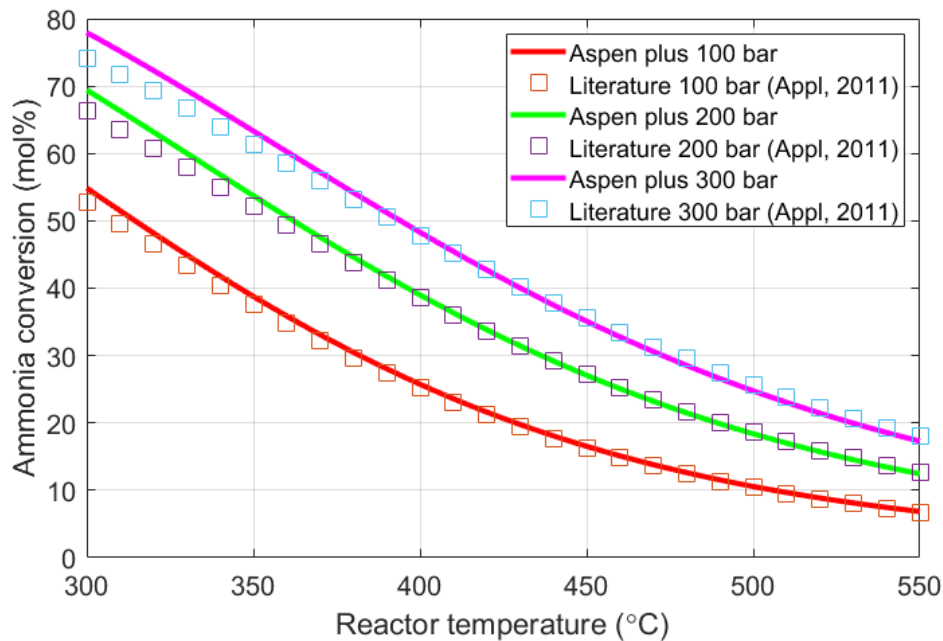


Figure 23. Validation of ammonia conversion of isothermal RGIBBS reactor.

5.2 Parametric simulation

The green ammonia plant is simulated to produce 213,1 kt/ NH_3 and 37,9 kt/ H_2 in the reference year 2024. Capacity factor of AEL is counted the be 80,6 % with the total PPA electricity generation capacity of 825 MW. Based on the process simulation, the plant can generate up to 115 MW of utilizable waste heat. Out of this, 23 MW is generated by the Haber-Bosch process, and the rest is generated by AEL. Table 11 presents the COP values of the heat pump in the different scenarios.

Table 11. COP values of the heat pump with different temperature lifts.

Temperature lift (°C)	COP
50	4,6
40	6,8
30	8,7

Figure 24 and figure 25 illustrate DH supply water temperature profiles of cities. In this chapter, figures are color-coded blue lines refer to Oulu and red lines to Kokkola. The weather in Oulu was colder than in Kokkola during the reference year. Resulting in a higher share of high-temperature DH demand. In Oulu, simulated high-temperature cases accounted for 13.7 % of the annual hours compared to 10.1 % in Kokkola. Thus, demonstrating better capacity factor for high temperature waste heat utilization in Oulu.

The electricity consumption of DH production illustrated in figure 26 and 28 is dominated by the heat pump since the Haber-Bosch side the pump maximum electric power is only 0,036 MW. Therefore, electricity consumption does not increase much during the high temperature cases. Highlighting the excellent feasibility to utilize this waste from technical perspective. The most influencing factor to electricity consumption is the required temperature lift in the heat pump. This explains the correlation between DH supply temperature and electricity consumption figures. There is heavy ramping up and down in electricity consumption and DH production profiles presented in this chapter. This ramping caused by fluctuation of renewable power. The zero values in both profiles are explained by the maintenance break when there is no waste heat available from the green ammonia plant. In figure 27 and figure 29, the highest DH production spikes updraws are caused by utilization the waste heat from Haber-Bosch process in the high temperature scenarios. In contrast, the lowest in DH production are caused by situation when the AEL is operated at minimum power.

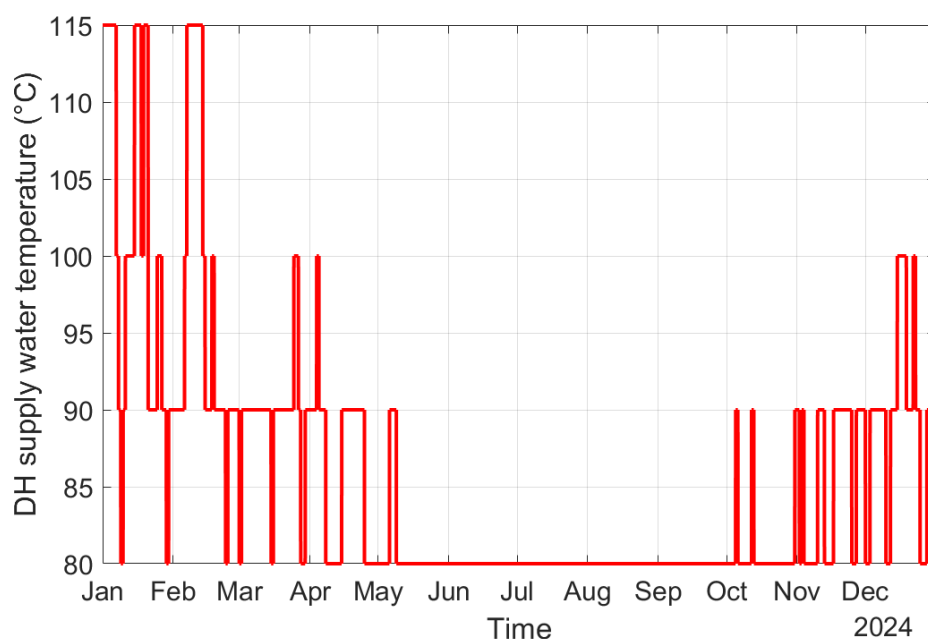


Figure 24. DH supply water temperature in Kokkola.

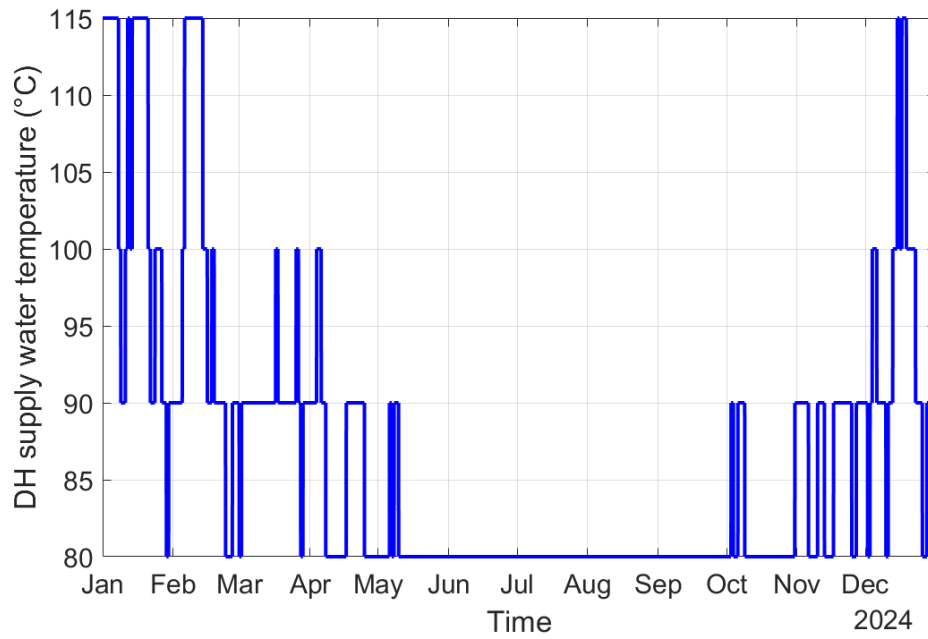


Figure 25. DH supply water temperature in Oulu.

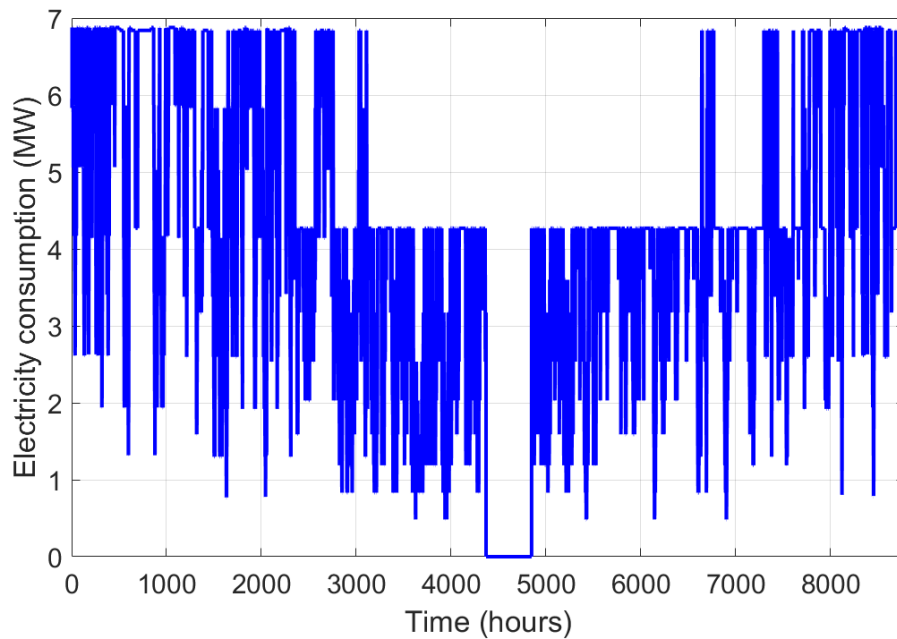


Figure 26. Electricity consumption of the plant DH system in Oulu.

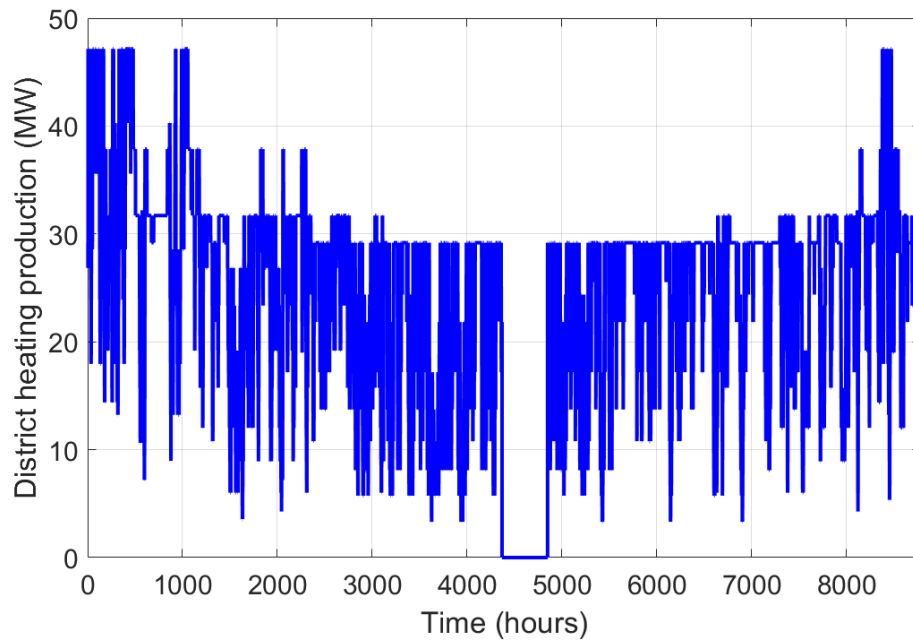


Figure 27. DH production of the plant in Oulu.

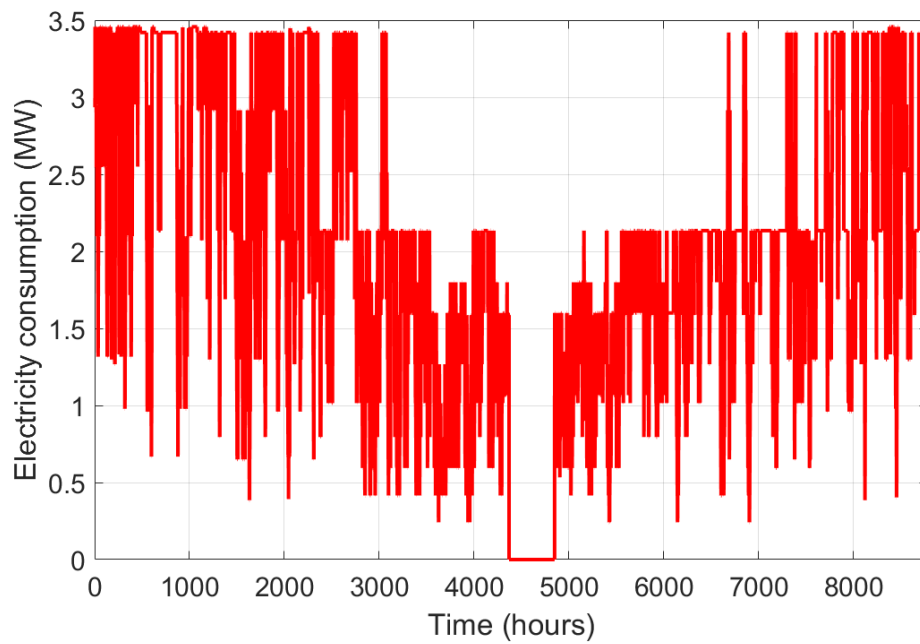


Figure 28. Electricity consumption of the plant DH system in Kokkola.

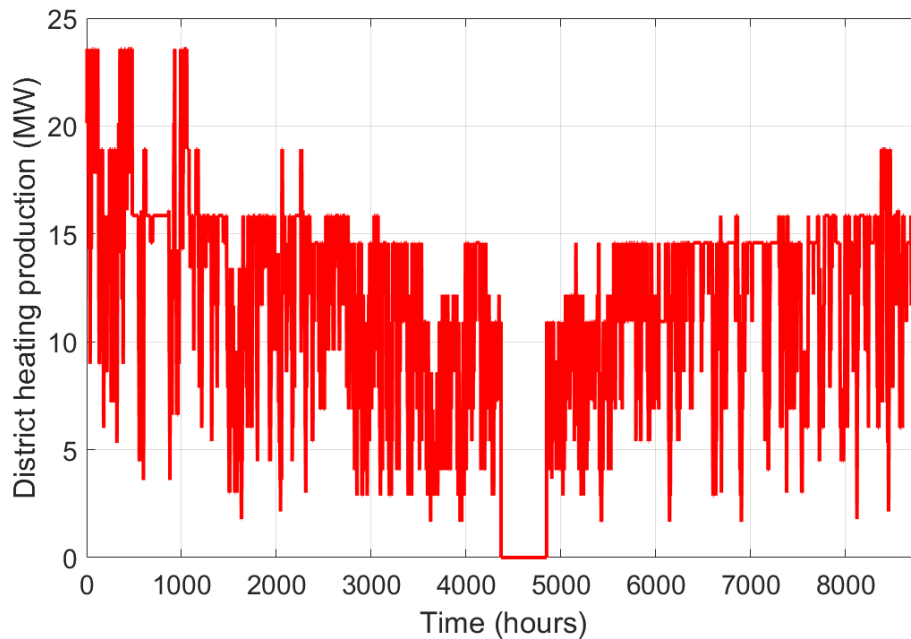


Figure 29. DH production of the plant in Kokkola.

Table 12 presents key results of simulated cities. Heat pump full load hour illustrates time annually when DH production does not exceed the demand. Overproduction of DH heating is only a problem in summer as can be expected due to low demand for DH. In Oulu, curtailment of the (DH) system is minimal since it occurs during only 0.16 % of annual hours. In Kokkola, curtailment is required around 12 % of the time.

The second special scenario occurs only in Oulu where it is more likely due to larger system. However, the second special scenario can occur in both cities since it depends on weather conditions, hydrogen feed rate into Haber-Bosch processes and storage level of hydrogen storage. This scenario occurs most likely in conditions when low renewable power generation leads low single stack power and hydrogen feed rate HB-Bosch process is also low. The flexibility of the Haber-Bosch process is the determining factor since the pure difference in mass flow between steam and water from heat pumps prevents DH water from being heated to the target temperature. This indicates that there is a limit for heat pump capacity depending on flexibility of the Haber-Bosch process and installed capacity of heat pump.

Table 12. Key numerical results of the parametric simulation.

Result	Oulu	Kokkola	Unit
Number of stacks connect into DH production	8/30	4/30	
Max DH production capacity	47,16	23,58	MW
Heat pump capacity	31,71	15,85	MWh _{th}
DH production	214,2	101,5	GWh/a
DH production electricity consumption	36,5	17,51	GWh/a
Curtailement in DH production annually	0,16	11,98	%/h
Desired DH target temperature cannot be achieved	16	0	h/a

In both cities, waste heat from the green ammonia is partly utilized in parametric simulation due selected objective function and system boundaries of this thesis. In Oulu, the heat pump system capacity is simulated to be double compared to Kokkola with 8 of 30 stack connected into DH production. The maximum DH production illustrates total DH production capacity including the steam utilization with given the number of stacks connected into DH production.

Full utilization is not a reasonable objective since this industrial-scale green ammonia plant is a very large waste heat source due to maximum utilizable waste heat output of 115 MW. Higher utilization rate of the waste heat would lead to high curtailement in heat pump system during summer months. Secondly, DH network cannot be dependent on a single heat source due for security of supply reasons. Hence, majority of the waste heat must be wasted into environment in order this investment to be feasible.

Higher utilization rate of the waste heat would require DH network with higher baseload consumption outside heating seasons or the implementation thermal energy storage. In theory, DH demand during summer can be covered by utilizing waste heat from the green ammonia plant by connecting more stacks to DH production and expanding the heat pump system in both cities

As conclusion, parametric simulation demonstrates that green ammonia plant is excellent source of waste heat for DH production due to high-capacity factor of AEL. Secondly, the plant always generates some waste heat except during annual maintenance. However, the low-capacity factor for high-temperature waste heat suggests alternative utilization strategies could be more feasible than the strategy examined in this thesis. One alternative is to utilize

the high-temperature waste heat to continuously raise DH water temperature. Alternatively, this heat could be utilized in other applications when it is not needed for DH production.

5.3 Levelized cost of heat

Table 13 illustrates results of sensitivity analysis of produced LCOH for both cities. The results show that levelised cost are heat are competitive even with higher discount rates. Although maximizing ammonia production is the optimization target in a green ammonia plant. The single largest CAPEX cost of the system is the heat pump followed by DH pipeline. LCOH of Oulu is lower than Kokkola due to economics of scale. Firstly, Haber-Bosch side components and DH pipeline cost assumed to be equal. Secondly, curtailment of the heat pump system is lower in Oulu where DH consumption larger and DH production exceeds more seldom the DH demand than in Kokkola. One influencing factor is also determined single heat pump size which influences to the sizing of the system. Thus, it also effects on the lifetime investment costs and energy production in LCOH equation. The heating capacity of single heat pump is 5,285 MW in both cities.

Table 13. Sensitivity analysis results of LCOH.

Discount rate (%)	Oulu	Kokkola	Unit
2	19,0	23,3	€/MWh
4	20,5	25,2	€/MWh
6	22,0	27,3	€/MWh
8	23,7	29,6	€/MWh
10	25,5	32,0	€/MWh
12	27,4	34,5	€/MWh

This waste heat source naturally avoids high electricity costs during price spikes, which occur whenever renewable power output declines heavily in the 2024 parametric simulation. During the expensive hours, both electrolyser power consumption and waste heat generation decrease which consecutively reduces the electricity consumption of the heat pumps. In addition, the electricity consumption of the DH pump associated with the Haber-Bosch process is magnitude lower than the heat pumps. Thus, it does not notably contribute to costs during the high supply temperature cases when DH demand

is high, and electricity price is also often high. Therefore, LCOH are competitive without optimization of heat production in both cities.

5.4 Electricity generation

Table 14 presents electricity generation results of utilization of high temperature waste heat from Haber-Bosch process. The results of table are simulated in Aspen Plus with hydrogen feed rate of 5252,6 kg/h into Haber-Bosch process which is the maximum hydrogen feed rate determined in this thesis. Q_{in} is a constant with every working fluid since heat extraction is limited by preheating of the syngas into the reactor. Hence, reducing the mass flowrate inside ORC cycle.

The results of table 14 indicate that ORC fluids are better alternatives than water with Rankine cycle due to better net work generation and thermal efficiency. Hence, ORC is better option for this scale green ammonia plant. The results obtained are better than in the reality since losses are not considered in this thesis. Simulated ORC fluids could cover from 61,7 % to 67,7 % of the Haber Bosch process electricity consumption as electricity consumption of the processes 9.41 MW at maximum hydrogen feed rate.

Table 14. Electricity generation results of different working fluids.

Result	Ben- zene	Tolu- ene	Cyclo- hexane	Water	Unit
W_{turbine}	6,59	6,45	6,02	5,91	MW
W_{pump}	0,22	0,17	0,21	0,12	MW
W_{net}	6,37	6,28	5,81	5,79	MW
Q_{in}	23,52	23,52	23,52	23,52	MW
n_t	27,1	26,7	24,7	24,6	%
$\frac{W_{\text{turbine}}}{P_{\text{Haber-Bosch}}}$	67,7	66,7	61,7 %	61,5	%

In general, the power generation is quite low since the turbine model used to simulate wind production in thesis has rated power of 6,6 MW which typical rated power for currently installed onshore wind turbines. On the other hand, the generated power could be utilized to improve self-sufficiency of a green ammonia plant by offsetting partly its electricity consumption. Second alternative is to utilize power to cover DH production electricity consumption. Kokkola, simulated net work generation is greater than the maximum electric power of heat pump system, which is 3,42 MW. Thus, power demand of heat pump could be covered if waste heat of AEL is only utilized to DH production. In Oulu, the maximum electric power of the heat pump system is 6,84 MW. In contrast, this value exceeds the net work generation potential of any the

examined working fluids. In the future, the potential imbalance between electricity generation and consumption should be investigated further since it may pose a significant drawback for electricity utilization in own usage. In addition, economic viability of own electricity generation is also a factor of uncertainty. Third alternative is of course to sell electricity to market.

The net power generation of all ORC fluids is within the typical range of the cycle. Nevertheless, load flexibility is a key factor in determining the extent to which waste heat can be effectively utilized particularly in green ammonia plants where the feed rate varies over time. Hence, load flexibility for ORC is greater than the Haber-Bosch process and this allows for sufficient utilization of waste heat.

5.5 Limitations of the thesis

The calculations are based on electricity prices, weather condition, renewable power data and DH consumption profiles from a single reference year. Therefore, it is not certain that upcoming years are similar as the reference year 2024. Another source of uncertainty in this thesis is the renewable energy production data. The dataset from Renewables.ninja does not account for potential icing of wind turbines. Thus, the simulated renewable power production might be higher during hours when icing occurs in the reality.

In the Aspen model, number of different scenarios is limited terms of power and DH supply temperature levels. A real green ammonia plant would more flexible. Similarly, nitrogen production excluded from thesis could impose limitations for the operating profile of the plant. Moreover, there is uncertainty related to modern Haber-Bosch process flexibility or possible ramping constrains in the literature. In this thesis, all ramping constrains are neglected which may result in unrealistic fluctuations in operation on hourly basis.

In the model, the maximum hydrogen production and the maximum hydrogen feed rate into Haber-Bosch model are assumed to be equal which is not certain in a real plant. Overall, the simulated plant operations are not optimized which is also affecting to DH production. In the LCOH calculations, the DH production system is considered as a price taker in the electricity market which has no impact on the spot price of electricity. However, this assumption might be invalid with MW scale system during the coldest periods when the electricity supply curve is usually very inflexible.

6 Conclusions

This thesis researched waste heat utilization from industrial scale green ammonia plant with 300 MW alkaline electrolyzer combined with Haber-Bosch process. The plant is modelled with Aspen Plus software and the parametric simulation of DH production is conducted in MATLAB code based on Aspen Plus model results. The aim of the thesis has been to simulate a production profile of a plant with annual production around 210 kt/NH₃. The focus in thesis have been investigate waste heat utilization in DH networks in Finland. However, potential for electricity generation from high-temperature waste heat is also demonstrated by process simulation calculations.

Literature review revealed that there are lot of different potential applications and industries for waste heat utilization. Industrial scale ammonia plant can be considered as very large waste heat source since in the maximum usable waste heat generation is calculated to be 115 MW. This magnitude heat source can be utilized most feasible by large heat consumer such as DH networks or green houses or combination of many heat consumers simultaneously. Green ammonia plants are planned to be constructed next to deep-water ports preventing economically feasible utilization in green houses located typically in rural areas. In general, the economic viability of waste heat utilization is highly dependent on minimizing transport distance.

The parametric simulation of DH production illustrated high fluctuation in DH production. However, generates always some waste heat for DH production expect during the maintenance break. The results indicated that partly utilization of the waste heat is the most feasible alternative in terms of avoiding curtailment of DH production. In Oulu system was sized with maximum heating power of 47,16 MW with only 0,2 %/h curtailment of the plant operational hours in DH production. In Kokkola, same values were 23,58 MW with 12 %/h curtailment. These results indicate that very reasonable heat pump sizing can be found for different size DH networks. However, the conducted scenario of the parametric simulation is not optimal due low-capacity factor of the high temperature waste heat utilization.

The full utilization of the waste heat is not feasible objective due to economic, and security of supply reasons related to DH networks. There are also limiting factors in depending on heat pumps system size and operation conditions after the DH water cannot be heated to needed temperature levels with steam from Haber-Bosch process. Furthermore, the pure scale of waste heat generation limits feasible utilisation especially in smaller DH networks.

Sensitivity analysis of LCOH showed that DH production is competitive with LCOH ranging from 19,0 €/MWh to 27,4 €/MWh in Oulu and from 23,3 €/MWh to 34,5 €/MW in Kokkola depending on applied discount rate. Heat pumps constituted the largest single CAPEX cost followed by DH pipeline. The larger city benefits from economies of scale, and Oulu also achieved lower curtailment value for DH production.

As conclusion, a green ammonia plant is excellent waste heat source and ammonia has vital role in fertilizer production enabling the modern agriculture. On the other hand, a green ammonia plant is an expensive investment, and green ammonia competes against other sustainable energy carriers. Furthermore, there are only a limited number of suitable locations available for a plant of this size in Finland.

The results of electricity generation processes simulations indicated that ORC is more feasible option than traditional Rankine cycle in terms of thermal efficiency and typical cycle generation capacity. However, the maximum net work output with the ORC is approximately 6,4 MW. The heat integration of the Haber-Bosch process limits amount of recoverable waste heat for power generation. In theory, electricity could be utilized to increase the self-sufficiency of the plant. Another interesting alternative would be to utilize own electricity generation to power heat pumps. Hence, the maximum electric power of the heat pump was 3,42 MW in Kokkola, while in Oulu it reached to 6,84 MW.

Green ammonia plants are still relatively new topic in scientific research. Therefore, there are many topics that should be researched. Based on findings of thesis, an interesting future research topic would be integration of thermal energy storage into the DH production system. Secondly, the potential for utilizing electricity generation to power heat pumps should be investigated in greater extend with a particular focus on analyzing the temporal mismatch between electricity production and consumption. Thirdly, cogeneration from high temperature waste heat should be researched to improve capacity factor of heat utilization. However, the most crucial topic would be to examine economic feasibility of electricity generation. Hence, it ultimately determines what is the most viable application for the waste heat.

References

- Adibi, T., Sojoudi, A. and Saha, S.C., 2022. Modeling of thermal performance of a commercial alkaline electrolyzer supplied with various electrical currents. *International Journal of Thermofluids*, 13, p.100126. <https://doi.org/10.1016/j.ijft.2021.100126>
- Araújo, A. and Skogestad, S., 2008. Control structure design for the ammonia synthesis process. *Computers & Chemical Engineering*, 32(12), pp.2920-2932. doi:10.1016/j.compchemeng.2008.03.001
- Anwar, M., Mehdizadeh, A. and Karimi, N., 2024. Waste heat recovery from a green ammonia production plant by Kalina and vapour absorption refrigeration cycles: A comparative energy, exergy, environmental and economic analysis. *Sustainable Energy Technologies and Assessments*, 69, p.103916. <https://doi.org/10.1016/j.seta.2024.103916>
- Appl, M., 2011. Ammonia, 2. production processes. Ullmann's encyclopedia of industrial chemistry. https://doi.org/10.1002/14356007.002_011
- Arpagaus, C., Bless, F., Uhlmann, M., Schiffmann, J. and Bertsch, S.S., 2018. High temperature heat pumps: Market overview, state of the art, research status, refrigerants, and application potentials. *Energy*, 152, pp.985-1010. <https://doi.org/10.1016/j.energy.2018.03.166>
- Bao, J. and Zhao, L., 2013. A review of working fluid and expander selections for organic Rankine cycle. *Renewable and sustainable energy reviews*, 24, pp.325-342. <http://dx.doi.org/10.1016/j.rser.2013.03.040>
- Bora, N., Singh, A.K., Pal, P., Sahoo, U.K., Seth, D., Rathore, D., Bhadra, S., Sevda, S., Venkatramanan, V., Prasad, S. and Singh, A., 2024. Green ammonia production: Process technologies and challenges. *Fuel*, 369, p.131808. <https://doi.org/10.1016/j.fuel.2024.131808>
- Brauns, J. and Turek, T., 2020. Alkaline water electrolysis powered by renewable energy: A review. *Processes*, 8(2), p.248. <https://doi.org/10.3390/pr8020248>
- Brückner, S., Liu, S., Miró, L., Radspieler, M., Cabeza, L.F. and Lävemann, E., 2015. Industrial waste heat recovery technologies: An economic analysis of heat transformation technologies. *Applied Energy*, 151, pp.157-167. <http://dx.doi.org/10.1016/j.apenergy.2015.01.147>

Buttler, A. and Spliethoff, H., (2018). Current status of water electrolysis for energy storage, grid balancing and sector coupling via power-to-gas and power-to-liquids: A review. *Renewable and Sustainable Energy Reviews*, 82, pp.2440-2454. <http://dx.doi.org/10.1016/j.rser.2017.09.003>

Cameli, F., Kourou, A., Rosa, V., Delikonstantis, E., Galvita, V., Van Geem, K.M. and Stefanidis, G.D., 2024. Conceptual process design and techno-economic analysis of an e-ammonia plant: Green H₂ and cryogenic air separation coupled with Haber-Bosch process. *International Journal of Hydrogen Energy*, 49, pp.1416-1425. <https://doi.org/10.1016/j.ijhydene.2023.10.020>

Cheema, I.I. and Krewer, U., 2018. Operating envelope of Haber–Bosch process design for power-to-ammonia. *RSC advances*, 8(61), pp.34926-34936. DOI: 10.1039/c8ra06821f

Cehade, G. and Dincer, I., 2021. Progress in green ammonia production as potential carbon-free fuel. *Fuel*, 299, p.120845. <https://doi.org/10.1016/j.fuel.2021.120845>

Collado, L., Pizarro, A.H., Barawi, M., García-Tecedor, M. and Liras, M., 2024. Light-driven nitrogen fixation routes for green ammonia production. *Chemical Society Reviews*. DOI: 10.1039/d3cs01075a

David, A., Mathiesen, B.V., Averfalk, H., Werner, S. and Lund, H., 2017. Heat roadmap Europe: large-scale electric heat pumps in district heating systems. *Energies*, 10(4), p.578. <https://doi.org/10.3390/en10040578>

David, M., Ocampo-Martínez, C. and Sánchez-Peña, R., 2019. Advances in alkaline water electrolyzers: A review. *Journal of Energy Storage*, 23, pp.392-403. <https://doi.org/10.1016/j.est.2019.03.001>

De la Hera, G., Ruiz-Gutiérrez, G., Viguri, J.R. and Galán, B., 2024. Flexible green ammonia production plants: Small-Scale simulations based on energy aspects. *Environments*, 11(4), p.71 <https://doi.org/10.3390/environments11040071>

Ebenhoch, R., Matha, D., Marathe, S., Muñoz, P.C. and Molins, C., 2015. Comparative levelized cost of energy analysis. *Energy Procedia*, 80, pp.108-122. doi: 10.1016/j.egypro.2015.11.413

ENTSO-E. European Network of Transmission System Operators for Electricity. Transparency platform. [Accessed 5 April 2025]. Available: <https://newtransparency.entsoe.eu/?appState=%7B%22sa%22%3A%5B%5D%2C%22st%22%3A%22BZ>

[N%22%2C%22mm%22%3Atrue%2C%22ma%22%3Afalse%2C%22sp%22%3A%22CLOSED%22%2C%22dt%22%3Anull%2C%22df%22%3Anull%2C%22tz%22%3A%22CET%22%7D](#)

EK. (2025). Confederation of Finnish Industries. Green investments in Finland. [Accessed 12 May 2025]. Available: <https://ek.fi/en/green-investments-in-finland/>

Fingrid. Grid service fees for 2025. [Accessed 6 May 2025]. Available: <https://www.fingrid.fi/globalassets/dokumentit/en/customers/grid-connection/grid-service-fees-2025.pdf>

Finlex. (2022). Ilmastolaki. 423/2022. Ministry of the Environment. [Accessed 12 May 2025]. Available: <https://finlex.fi/eli?uri=http://data.finlex.fi/eli/sd/2022/423/ajantasa/2024-12-19/fin>

Finnish Energy. (2024). Statistics on district heating. Energy Year 2024. [Accessed 22 April 2025]. Available: <https://energia.fi/en/statistics/statistics-on-district-heating/>

Finnish Energy DH Networks. (2024). District heating networks. [Accessed 22 April 2025]. Available: <https://energia.fi/en/energy-sector-in-finland/energy-networks/district-heating-networks/>

Finnish Energy statistics (2024). DH Networks construction cost. [Accessed 6 MAY 2025]. Available: <https://energia.fi/tilastot/kaukolampojohtojen-arakentamiskustannukset/>

Finnish Meteorological Institute. Havaintojen lataus. [Accessed 29 April 2025]. Available: <https://www.ilmatieteenlaitos.fi/havaintojen-lataus>

Gillespie, L.J. and Beattie, J.A., 1930. The thermodynamic treatment of chemical equilibria in systems composed of real gases. I. An approximate equation for the mass action function applied to the existing data on the Haber equilibrium. *Physical review*, 36(4), p.743. <https://doi.org/10.1103/PhysRev.36.743>

Green North Energy Oy. (2023). Green ammonia plant environmental impact assessment Naantali. [Accessed 6 May 2025]. Available: <https://www.ymparisto.fi/fi/osallistu-ja-vaikuta/ymparistovaikutusten-arviointi/green-north-energy-oy-vihrean-vedyn-ja-ammoniakin-tuotantolaitos-naantali>

Grosse, R., Christopher, B., Stefan, W., Geyer, R. and Robbi, S., 2017. Long term (2050) projections of techno-economic performance of large-scale heating and cooling in the EU. EUR28859. Publications Office of the European Union, Luxembourg, 2017. doi:10.2760/24422,

Helen. Kaukolämpölaiteet. [Accessed 16 June 2025]. Available: <https://www.helen.fi/yriyukset/lampoa-yriyksille/tietoa-yriytysasiakkaalle/kaukolampolaitteet>

Hu, B., Wu, D., Wang, L.W. and Wang, R.Z., 2017. Exergy analysis of R1234ze (Z) as high temperature heat pump working fluid with multi-stage compression. *Frontiers in Energy*, 11, pp.493-502. <https://doi.org/10.1007/s11708-017-0510-6>

IEA, I., Steel technology Roadmap, Paris [Accessed 8 April 2025] Available at: <https://www.iea.org/reports/iron-and-steel-technology-roadmap>

Jensen, J.O., Vestbø, A.P., Li, Q. and Bjerrum, N.J., 2007. The energy efficiency of onboard hydrogen storage. *Journal of Alloys and Compounds*, 446, pp.723-728. DOI: 10.1016/j.jallcom.2007.04.051

Jiménez-García, J.C., Ruiz, A., Pacheco-Reyes, A. and Rivera, W., 2023. A comprehensive review of organic rankine cycles. *Processes*, 11(7), p.1982. <https://doi.org/10.3390/pr11071982>

Karellas, S., Leontaritis, A.D., Panousis, G., Bellos, E. and Kakaras, E., 2013. Energetic and exergetic analysis of waste heat recovery systems in the cement industry. *Energy*, 58, pp.147-156. <http://dx.doi.org/10.1016/j.energy.2013.03.097>

Kosmadakis, G., 2019. Estimating the potential of industrial (high-temperature) heat pumps for exploiting waste heat in EU industries. *Applied Thermal Engineering*, 156, pp.287-298. <https://doi.org/10.1016/j.applthermaleng.2019.04.082>

Kumar, S. Shiva, and VJMSfET Himabindu. "Hydrogen production by PEM water electrolysis—A review." *Materials Science for Energy Technologies* 2, no. 3 (2019): 442-454. <https://doi.org/10.1016/j.mset.2019.03.002>

Lange, H., Klose, A., Lippmann, W. and Urbas, L., 2023. Technical evaluation of the flexibility of water electrolysis systems to increase energy flexibility: A review. *International Journal of Hydrogen Energy*, 48(42), pp.15771-15783. <https://doi.org/10.1016/j.ijhydene.2023.01.044>

Lin, B., Wiesner, T. and Malmali, M., 2020. Performance of a small-scale Haber process: A techno-economic analysis. *ACS Sustainable Chemistry & Engineering*, 8(41), pp.15517-15531 <https://dx.doi.org/10.1021/acssuschemeng.0c04313>

Lohmann-Richters, F. P., S. Renz, W. Lehnert, Martin Müller, and M. Carmo. "challenges and opportunities for increased current density in alkaline electrolysis by increasing the operating temperature." *Journal of The Electrochemical Society* 168, no. 11 (2021): 114501. DOI 10.1149/1945-7111/ac34cc

Lund, H., Østergaard, P.A., Nielsen, T.B., Werner, S., Thorsen, J.E., Gudmundsson, O., Arabkoohsar, A. and Mathiesen, B.V., 2021. Perspectives on fourth and fifth generation district heating. *Energy*, 227, p.120520. <https://doi.org/10.1016/j.energy.2021.120520>

Mariani, L., Cola, G., Bulgari, R., Ferrante, A. and Martinetti, L., 2016. Space and time variability of heating requirements for greenhouse tomato production in the Euro-Mediterranean area. *Science of the Total Environment*, 562, pp.834-844. <http://dx.doi.org/10.1016/j.scitotenv.2016.04.057>

Mazhar, A.R., Liu, S. and Shukla, A., 2018. A state of art review on the district heating systems. *Renewable and Sustainable Energy Reviews*, 96, pp.420-439. <https://doi.org/10.1016/j.rser.2018.08.005>

Meriläinen, A., Kosonen, A., Jokisalo, J., Kosonen, R., Kauranen, P. and Ahola, J., 2024. Techno-economic evaluation of waste heat recovery from an off-grid alkaline water electrolyzer plant and its application in a district heating network in Finland. *Energy*, 306, p.132181. <https://doi.org/10.1016/j.energy.2024.132181>

Morgan, E.R., Manwell, J.F. and McGowan, J.G., 2017. Sustainable ammonia production from US offshore wind farms: a techno-economic review. *ACS Sustainable Chemistry & Engineering*, 5(11), pp.9554-9567. <https://doi.org/10.1021/acssuschemeng.7b02070>

Nguyen, T.Q., Slawnwhite, J.D. and Boulama, K.G., 2010. Power generation from residual industrial heat. *Energy Conversion and Management*, 51(11), pp.2220-2229. doi:10.1016/j.enconman.2010.03.016

OX2. Lestijärvi. [Accessed 25 April 2025]. Available: <https://www.ox2.com/fi/suomi/hankkeet/lestijarvi/>

Pethurajan, V., Sivan, S. and Joy, G.C., 2018. Issues, comparisons, turbine selections and applications—An overview in organic Rankine cycle. *Energy*

conversion and management, 166, pp.474-488.
<https://doi.org/10.1016/j.enconman.2018.04.058>

Pezzuolo, A., Benato, A., Stoppato, A. and Mirandola, A., 2016. The ORC-PD: A versatile tool for fluid selection and Organic Rankine Cycle unit design. *Energy*, 102, pp.605-620. <http://dx.doi.org/10.1016/j.energy.2016.02.128>

Osman, O., Sgouridis, S. and Sleptchenko, A., 2020. Scaling the production of renewable ammonia: A techno-economic optimization applied in regions with high insolation. *Journal of cleaner production*, 271, p.121627. <https://doi.org/10.1016/j.jclepro.2020.121627>

Rahbar, K., Mahmoud, S., Al-Dadah, R.K., Moazami, N. and Mirhadizadeh, S.A., 2017. Review of organic Rankine cycle for small-scale applications. *Energy conversion and management*, 134, pp.135-155. <http://dx.doi.org/10.1016/j.enconman.2016.12.023>

Rayegan, R. and Tao, Y.X., 2011. A procedure to select working fluids for Solar Organic Rankine Cycles (ORCs). *Renewable Energy*, 36(2), pp.659-670. doi:10.1016/j.renene.2010.07.010

Renewables Finland. Project map of renewable energy Forms. [Accessed 25 March 2025]. Available: <https://suomenuusiutuvat.fi/en/wind-power/projects-and-wind-turbines-in-finland/wind-power-map/>

Renwables.ninja. [Accessed 25 March 2025]. Available: <https://www.renewables.ninja/> <https://doi.org/10.1016/j.energy.2016.08.060> & <https://doi.org/10.1016/j.energy.2016.08.068>

Rouwenhorst, K.H., Travis, A.S. and Lefferts, L., 2022. 1921–2021: A Century of renewable ammonia synthesis. *Sustainable Chemistry*, 3(2), pp.149-171. <https://doi.org/10.3390/suschem3020011>

Ruddock, J., Short, T.D. and Brudenell, K., 2003. Energy integration in ammonia production. *WIT Transactions on Ecology and the Environment*, 62. ISSN 1743-3541

Saari, A. and Sekki, T., 2008. Energy consumption of a public swimming bath. *The Open Construction and Building Technology Journal* 2 (2008) 202–206. DOI: 10.2174/1874836800802010202

Sakas, G., Ibáñez-Rioja, A., Ruuskanen, V., Kosonen, A., Ahola, J. and Bergmann, O., 2022. Dynamic energy and mass balance model for an industrial

alkaline water electrolyzer plant process. *International Journal of Hydrogen Energy*, 47(7), pp.4328-4345. <https://doi.org/10.1016/j.ijhydene.2021.11.12>

Salmon, N. and Bañares-Alcántara, R., 2022. A global, spatially granular techno-economic analysis of offshore green ammonia production. *Journal of Cleaner Production*, 367, p.133045. <https://doi.org/10.1016/j.jclepro.2022.133045>

Sánchez, M., Amores, E., Abad, D., Rodríguez, L. and Clemente-Jul, C., 2020. Aspen Plus model of an alkaline electrolysis system for hydrogen production. *International journal of hydrogen energy*, 45(7), pp.3916-3929. <https://doi.org/10.1016/j.ijhydene.2019.12.027>

Smith, C., Hill, A.K. and Torrente-Murciano, L., 2020. Current and future role of Haber–Bosch ammonia in a carbon-free energy landscape. *Energy & Environmental Science*, 13(2), pp.331-344. DOI: 10.1039/C9EE02873K

Sunfire. (2024). Sunfire-Hylink Alkaline. [Accessed 11 March 2025]. Available: <https://backend.sunfire.de/wp-content/uploads/2024/10/Sunfire-Fact-Sheet-AEL-EN-digital.pdf>

Ursua, A., Gandia, L.M. and Sanchis, P., 2011. Hydrogen production from water electrolysis: current status and future trends. *Proceedings of the IEEE*, 100(2), pp.410-426. DOI: 10.1109/JPROC.2011.2156750.

van der Roest, E., Bol, R., Fens, T. and van Wijk, A., 2023. Utilisation of waste heat from PEM electrolyzers–Unlocking local optimisation. *international journal of hydrogen energy*, 48(72), pp.27872-27891. <https://doi.org/10.1016/j.ijhydene.2023.03.374>

Vero. (2025). Electricity tax. [Accessed 6 May 2025]. Available: <https://www.vero.fi/yriytykset-ja-yhteisot/verot-ja-maksut/valmistevero-tus/sahkovero/>

Wang, S., Zhang, P., Zhuo, T. and Ye, H., 2023. Scheduling power-to-ammonia plants considering uncertainty and periodicity of electricity prices. *Smart Energy*, 11, p.100113. <https://doi.org/10.1016/j.segy.2023.100113>

Witkowski, K., Haering, P., Seidelt, S. and Pini, N., 2020. Role of thermal technologies for enhancing flexibility in multi-energy systems through sector coupling: technical suitability and expected developments. *IET Energy Systems Integration*, 2(2), pp.69-79. <https://doi.org/10.1049/iet-esi.2019.0061>

Zhang, J., Zhang, H.H., He, Y.L. and Tao, W.Q., 2016. A comprehensive review on advances and applications of industrial heat pumps based on the practices in China. *Applied Energy*, 178, pp.800-825. <http://dx.doi.org/10.1016/j.apenergy.2016.06.049>

Zhang, K., Liang, X., Wang, L., Sun, K., Wang, Y., Xie, Z., Wu, Q., Bai, X., Hamdy, M.S., Chen, H. and Zou, X., 2022. Status and perspectives of key materials for PEM electrolyzer. *Nano Res. Energy*, 1(3), p.e9120032. <https://doi.org/10.26599/NRE.2022.9120032>

Appendix

Table 15. Electricity generation model specifications.

	Ben- zene	Tolu- ene	Cyclo- hexane	Wa- ter	Unit
Evaporator pressure	40,0	33,0	36,0	111,3	bar
Condenser pressure	0,14	0,051	0,14	1,00	bar
Superheating degree	0,0	0,0	0,0	135	°C
Condenser temperature	25,0	25,0	25,0	25,0	°C
Turbine outlet tempera- ture	94,0	138,0	133,0	100,0	°C
Vapor content after tur- bine	1,0	1,0	1,0	90	%

```
if avgTemp < -14
    heatingSetpoint = 115;
elseif avgTemp < -6
    heatingSetpoint = 100;
elseif avgTemp < 2
    heatingSetpoint = 90;
else
    heatingSetpoint = 80;
end
```

Figure 30. Logic of behind DH supply temperature values.